KERNFORSCHUNGSZENTRUM

KARLSRUHE

Oktober 1966

KFK 472

Institut für Angewandte Reaktorphysik

Initial Experiments in the Karlsruhe Fast Critical Facility, SNEAK

P. Engelmann, R. Böhme, G. Bruhn, R. Durand-Smet, W.K. Foell, F.W.A. Habermann, R. Schröder, D. Wintzer

GESELLSCHAFT FÜR KERNFORSCHUNG M.B.H.

KARLSRUHE

Gesellschaft für Kernforschung m.b.H.

Karlsruhe

KERNFORSCHUNGSZENTRUM KARLSRUHE

Okt. 1966 KFK-472

Institut für Angewandte Reaktorphysik

Initial Experiments in the Karlsruhe Fast Critical Facility, SNEAK*)

P. ENGELMANN, R. BÖHME, G. BRUHN, R. DURAND-SMET**), W.K. FOELL
F.W.A. HABERMANN***), R. SCHRÖDER, D. WINTZER

Gesellschaft für Kernforschung m.b.H., Karlsruhe

*) Work performed within the association in the field of fast reactors between the European Atomic Energy Community and Gesellschaft für Kernforschung mbH., Karlsruhe

**) INDATOM-EURATOM-Delegate

***) EURATOM-Delegate

1. Introduction

The experimental program of SNEAK is starting with measurements on a well-known fast uranium core, a repeat of the ZPR-3 assembly 41. This assembly has been chosen because all materials necessary for its simulation are already available at SNEAK. The purpose of "SNEAK 1" is to test the SNEAK facility and its experimental equipment. The data obtained will be compared with those of ZPR-3.

In support of the fast reactor development work at Karlsruhe, the next two assemblies are designed to investigate special features of sodium- and steam-cooled fast plutonium oxide reactors. Preparations for the sodium assembly "SNEAK 2" began in 1964, and for the steam assembly "SNEAK 3" in 1965.

In the meantime a number of experiments with dilute sodium-cooled systems have been performed in the USA and in the UK, partly also with plutonium fuel. However, information on steam-cooled fast reactor systems with plutonium fuel is still scare. Therefore the SNEAK program has been modified so that SNEAK 3 will be built before SNEAK 2. It is planned that mock-ups of sodium- and steam-cooled fast prototype reactors will follow these initial assemblies.

In this paper we will discuss some problems arising in the simulation of fast power reactors, preparations for sodium-void experiments, steam reactivity effect measurements, Doppler experiments, and a proposed mock-up for simulating the fission products in SNEAK. Other experiments such as spectrum-, breeding ratio-, noise-, and material worth measurements will not be discussed in this paper.

2. Problems of Simulating Power Reactors

Problems of simulation in SNEAK arise from the following facts:

1. At present only 175 kg of plutonium are available.
2. The plutonium used in SNEAK has a far lower Pu240 isotopic content (8%) than is characteristic for fast power reactor fuel (20-30%).
3. The SNEAK fuel contains no fission products.
4. Some limitations exist in the availability of non-fissile materials.
5. All core materials are in the form of plates.
6. SNEAK will operate at room temperature.

Each of these problems is discussed briefly below.

1. The shortage of plutonium fuel leads to the necessity of carrying out all experiments in U-Pu fueled assemblies. For the assemblies 2 and 3 we have chosen to separate the uranium and plutonium in order to obtain a plutonium zone with the appropriate composition. The remaining part of the core will be fueled by U235. To obtain "local correspondence" /1/ and good spectral matching with the plutonium cores of interest, the uranium driver zones are made of almost the same size and composition as the plutonium zones they replace. Criticality is achieved by adjusting the enrichment of the driver. For each measurement the shape of the plutonium zone has to be chosen in a way which minimizes the error introduced by the uranium driver zone. For central reactivity-, Doppler-, and spectrum measurements, a central plutonium zone will be surrounded by the uranium driver. The linear dimensions and the statistical weight of the plutonium zone are greatest in this geometry. For other experiments such as local void measurements, where the plutonium zone must be representative of the whole core, it will have the shape of a half cylinder or a sector. Details of the arrangements will be discussed in the following chapters.

2. An extreme case of zone loading will be used to study the influence of Pu^{240} on the reactivity change caused by loss of coolant or by flooding of the core of a steam-cooled fast reactor. Only very little plutonium containing the appropriate amount of Pu^{240} will be available. It will be used to build a small test zone with the correct Pu^{240} concentration and surrounded by a zone with a lower Pu^{240} content. To limit the size of the test zone a differential method will be used for the determination of the steam density coefficient of reactivity (SDC).

3. A third limitation is the lack of fission products in the SNEAK fuel. The effects of fission products are most pronounced in a soft spectrum; in a steam-cooled fast reactor of average burnup, the presence of fission products may add more than 1% Δk to the reactivity change due to loss of coolant. A fission product mock-up without highly radioactive isotopes has been designed. It allows the determination of fission product effects on various reactor parameters with relatively good accuracy. Composition and properties of the mock-up will be discussed in section 6.

4. In addition to the problems arising from the fuel and fission products, there are also problems in the simulation of other reactor materials. Several of them, e.g., sodium and oxygen, are not available at SNEAK in sufficient quantities to simulate an entire power reactor core. Outside the test zones these materials will be replaced by other materials with similar properties. Our calculations show that spectrum deviations between SNEAK and the simulated power reactor core can be minimized by simulating a single element by a mixture of suitably chosen elements. If, for example, two elements are chosen, the composition of the mixture is determined by two independent criteria. The errors introduced in the neutron spectrum by one element can to some extent be compensated by the other element. We took as a first condition that the average macroscopic degradation cross

sections of the reactor element and the simulating mixture be equal. As a second condition we required the equality of the degradation cross sections in that part of the spectrum of special importance for the measurements. Alternatively one may impose as a second condition the equality of the average transport cross sections.

5. Several steps have been taken to reduce the heterogeneity effects resulting from the plate structure of the core materials, e.g., diluting the U235 and Pu239 with U238, and using the plutonium as mixed Pu-U oxide. Nevertheless, in some experiments, heterogeneity effects will become important. For instance, the experiments to determine reactivity effects due to changes in coolant densities at various Pu240 concentrations must be corrected for heterogeneity effects. In some cases the heterogeneity corrections are of the same order of magnitude as the effects to be measured. From a phenomenological point of view, one can divide the heterogeneity effects into three types: a) Effects due to the high energy flux-peaking in the fuel plates, b) Effects due to increased resonance self-shielding in the eV and keV region, and c) Increase of the mean diffusion constant due to differences in the transport cross sections in the various plates. The effects of type b) are not very important in sodium-cooled fast reactors, but they play a major role in steam-cooled system. In the latter, the net heterogeneity effect depends on steam density and leads to large corrections to the void coefficient. In the flooded reactor, effects a) and b) lead to reactivity gains of the order of 5 to 10% in k. For this reason, heterogeneity investigations will receive more emphasis in SNEAK 3. The primary purpose of the investigations is to obtain experimental information about each of the three types of heterogeneity effects in order to test our calculational techniques.

6. The difference between the temperature of the zero power experiment and a power reactor leads to changes in material densities and changes in the resonance line shapes. The former effect does not cause problems because the density can be adjusted. The change of reactor parameters due to the latter effect can be estimated from Doppler effect measurements /2/.

3. Sodium Void Experiments

The objective of the assembly SNEAK 2 is to check reactor physics calculations in a system similar to a 300 MWe sodium-cooled prototype reactor. Emphasized are measurements concerning sodium safety coefficients /3/.

3.1 Calculational Reactor Model

A number of one- and two-dimensional diffusion calculations have been carried out in order to determine the restrictions imposed on the experiments by some of the limitations mentioned in section 2. The characteristics of the reactor model are shown in table 1.

Table 1: Reactor Model

Core diameter and height	128.64	cm
Reflector thickness	40	cm
Core volume	1670	l

Composition:

	Core	Driver	Reflector
Na	45%	45%	30%
Fe	25%	25%	22%
Fuel	30%	30%	48%
	(UO_2/PuO_2=5/1)	(21.3% enrichment)	(UO_2)

The fuel enrichment in the driver is adjusted so that the critical size of the reactor is not changed if part of the plutonium core is replaced by the uranium driver. In the driver zone 50% of the sodium and all of the oxygen are simulated by a suitable mixture of graphite and aluminium. This is possible without notably affecting measurements in the reactor center; the neutron fluxes change by less than 1%, the sodium danger coefficient by 2%, and the Doppler coefficient by only 1%.

Two shielded cross section sets were used for the calcualtions: The Russian ABN set /4/ and the German KFK set/5/, each with the same 26 group structure. A comparison with experimental results of ZPR-6 showed that the KFK set gives somewhat better agreement with experimental critical masses and spectral indices, but the ABN set gives better values for sodium coefficients.

3.2 Restricted Size of Experimental Zone

Measurements of the sodium void effect in the entire reactor core require large amounts of materials, a large excess reactivity, and much time for complete reloading of the core. However, in order to obtain values for sodium coefficients in the entire reactor it is not necessary to extend the measurements over the whole reactor. One may restrict such measurements to a 90° sector of half core height, as may be seen from the following results of some two-dimensional calculations in R-ϑ geometry.

Table 2: Reactivity Due to Sodium Voiding in All-Plutonium Core; Error of Sector Experiments

		Cross section set	
		ABN	KFK
Voiding of entire reactor core	Δk_{total}	$-1752 \cdot 10^{-5}$	$-652 \cdot 10^{-5}$
Error in Δk_{eff} sodium void:			
voiding of $\frac{1}{8}$ core	$\frac{1}{8}\Delta k_{total} - (\Delta k)_{\frac{1}{8}}$	$14 \cdot 10^{-5}$	$18 \cdot 10^{-5}$
" " $\frac{1}{4}$ core	$\frac{1}{4}\Delta k_{total} - (\Delta k)_{\frac{1}{4}}$	$13 \cdot 10^{-5}$	$22 \cdot 10^{-5}$
" " $\frac{1}{2}$ core	$\frac{1}{2}\Delta k_{total} - (\Delta k)_{\frac{1}{2}}$	$10 \cdot 10^{-5}$	$22 \cdot 10^{-5}$

The error made by restricting an experiment to a core sector of an all-plutonium reactor, even if the sector measures only 1/8 of the core, is practically constant and much smaller than the discrepancy between the results of the two cross section sets. This is caused by the fact that the flux variations in the boundary region have already reached their asymptotic form in such a small sector (fig. 1). By performing two measurements, one with 1/8 of the core, the other one with 1/4 of the core, one can eliminate the boundary error experimentally. The difference of the results of the two measurements gives exactly 1/8th of the sodium void effect of the entire reactor core. Calculations in slab geometry show that one may reduce the experimental zone in axial direction to 1/2 of the core height with negligible error ($\approx 2 \cdot 10^{-5}$).

3.3 Influence of the Uranium Driver

If the entire plutonium inventory of 175 kg is placed in a central zone with a radius of 42 cm (355 l volume) of the 1670 l reactor (table 1), the central sodium danger coefficient differs by only 2% from the central coefficient measured in the full plutonium reactor. If the radius of the central voided zone is increased to 31 cm (142 l volume) the difference becomes 14%. The max. positive reactivity change due to sodium voiding is achieved in a central zone with a radius less than 30 cm. Therefore it is possible, even with the small amount of plutonium fuel available, to measure the maximum positive void reactivity with sufficient accuracy.

Fig. 2 shows the mean value of the axial sodium danger coefficient as a function of the radius of the plutonium test zone. It is seen that the radius should be about 40 cm or larger in order that the influence of the driver on the axial sodium coefficient be negligible.

The error in sodium void measurements in extended core zones which is introduced by a uranium driver in the largest part of the core has been studied with one- and two-dimensional diffusion calculations (fig. 3). A sodium void experiment is assumed to be performed in a plutonium zone consisting of a core sector comprising 9/39 of the core. The rest of the core consists of the uranium driver and a variable plutonium zone adjacent to the experimental sector. The following sodium void effects in the experimental sector are calculated in R-Θ geometry with the KFK set condensed into 5 energy groups for the cases a through d of fig. 3.

Table 3: Sector Experiments in Pu-U Core

Case of fig. 3	Amount of Pu(kg) in variable Pu zone	Na void effect in fixed experimental sector ($10^{-3}\Delta k/k$)	error (%)
a	587	-1.73	(ref.)
b	78	-2.42	40
c	156	-2.14	24
d	144	-2.07	20

An analogous study has been performed in axial direction, assuming that the experimental zone is limited to the top half of the core. The bottom half contains a plutonium zone of variable thickness (fig. 3, cases e through h). The 40 cm thick reflector is not shown in the diagrams.

Table 4: Effect of Uranium Driver in Lower Core-Half

Case of fig. 3	Amount of Pu(kg) in variable Pu zone	KFK set (5 group)		ABN set (5 group)	
		Na void in upper half of core ($10^{-3}\Delta k/k$)	error %	Na void in upper half of core ($10^{-3}\Delta k/k$)	error %
e	381.5	-3.94	-	-9.58	(ref.)
f	91.5	-4.40	11.6	-10.41	8.7
g	46	-4.83	22.6	-10.81	12.7
h	0	-5.73	45.5	-11.46	19.6

With the amount of plutonium available, a combination of cases d and g appears to be a reasonable configuration for determining the sodium void effect of the all-plutonium core.

3.4 Influence of Reflector Composition

The reflector composition has practically no influence on the central sodium coefficient; it changes by only 1.3% if the breeder reflector of table 1 is replaced by a predominantly U238 reflector.

The influence of the axial reflector composition on the sodium coefficient in a core zone of 10 cm thickness adjacent to the reflector is shown in fig. 4. A gradually increasing amount of reflector, starting from the outside, has been replaced by U238. It is seen that the reflector composition has a rather large influence on the neighbouring core zone. One should exactly simulate the reflector over its full thickness in the vicinity of the reactor axis.

In the case of sector experiments the reflector should have breeder composition in the region adjacent to the experimental sector. Replacement of the breeder reflector by U238 elsewhere introduces an relative error of only 2% in the measured sodium void effect.

3.5 Sodium Void Experiments in Assembly 2

The assembly SNEAK 2 has been designed on the basis of the foregoing considerations.

The 1380 liter assembly (figs. 5 and 6) has the following composition: 38 ^{v}/o fuel (UO_2/PuO_2), 40 ^{v}/o Na, and 22 ^{v}/o SS.

The central 326 liter zone contains 165 kg plutonium with 8% Pu240 and 0.8% Pu241. The equivalent enrichment (ratio of fissile plutonium in this zone to all plutonium and uranium) is 0.15. The rest of the core consists of a uranium driver zone with the same volumetric compositions as the plutonium zone. The fuel enrichment in this zone is 0.19 (620 kg U235).

Central sodium void measurements include: 1) danger coefficient measurements, and 2) measurements in central zones of increasing size in order to determine the maximum positive sodium void effect. In addition, axial sodium void measurements are planned with the use of the pile oscillator. In order to perform these latter measurements in the upper core-half, the fuel elements containing plutonium are reloaded in such a way that the plutonium zone is located at the upper part of the core.

A measurement in a 1/8 core sector is proposed for determination of the sodium void effect in an entire plutonium core (fig. 6). This sector is far enough away from the uranium driver that no spectrum distortions occur at its surface. Calculations show, however, that a correction of 30% must be applied in order to account for the difference between the sodium void effect in the selected 1/8 SNEAK core sector and 1/8 of the sodium void effect in a complete plutonium core. This difference is due to the influence of the driver on the spectrum and its adjoint in the whole volume of the experimental plutonium sector (see section 4). Despite the relatively large corrections it seems possible, even with the small amount of plutonium fuel available at present, to determine the sodium void reactivity effects with an accuracy that is sufficient for the safety evaluation of the prototype reactor.

4. Measurements of Steam Density Coefficients of Reactivity in SNEAK 3

4.1 Experimental Program

In order to investigate the characteristics of a fast steam-cooled reactor, a critical assembly is proposed with a core volume of about 700 l and oxide fuel with a ratio $PuO_2/UO_2 = 1/6$.

Table 5 shows the composition of SNEAK 3. A unit cell of the core, built up of SNEAK plates and nickel tubes, is shown in fig. 7. This arrangement of tubes was chosen in order to facilitate measurements of the steam density coefficient of reactivity (SDC), i.e., the reactivity change per unit density change throughout the entire core. The nickel tubes run axially through the whole core and the upper axial blanket. Since no steam or water can be used in SNEAK for safety reasons, polyethylen will be used to simulate the steam. Polyethylene strings of varying diameter fill the central channels of the nickel tubes. These strings can easily be inserted or removed without unloading the plates.

A part of the reflector of the experimental reactor will be similar to a low density breeder blanket. However, most of the outer surface of the core will be reflected by a high density blanket of depleted uranium.

One possible version of assembly SNEAK 3 is shown in fig. 8. The cylindrical core will have a height of 90 cm and a diameter of 100 cm. The inner zone, surrounded by a uranium driver, has a height of 65 cm and a diameter of 72 cm, and is plutonium fueled. The mass of fissile material in the two zones is 142 kg Pu^{239} and 341 kg U^{235} respectively. The core will be surrounded by a blanket of 30 cm thickness.

A comparison of the neutron energy spectra of the plutonium and uranium reactors (fig. 9) indicates that the spectrum in the uranium zone would be somewhat harder than the spectrum of the plutonium zone. More striking are the discrepancies in the adjoint spectra (fig. 10). This will be of major importance for the SDC experiments.

The experimental program of SNEAK 3 is aimed primarily towards the investigation of:

a) The SDC and the coolant loss reactivity.

b) The influence of poisons, e.g., Pu^{240} and fission products, on the SDC.

c) The Doppler coefficient.

d) Material replacement coefficients, e.g., those of oxygen and structural materials.

e) Heterogeneity effects on the neutron energy spectrum, the reactivity, and the SDC.

Table 5: Composition of SNEAK 3

(Atom densities in units of 10^{20} cm^{-3})

Isotope	Plutonium Zone	Uranium Zone	Breeder Blanket
Pu239	13.41		
Pu240	1.20		
Pu241	0.12		
Pu242	0.01		
U235	0.58	19.15	0.7
U238	81.54	81.42	100.0
Cr	19.05	46.99	11.5
Fe	76.89	160.9	41.1
Ni	85.52	23.05	64.3
Al		71.20	71.2
C	0.28	47.89	47.9
O fuel	133.3	106.8	107.0
O steam	8.6	8.6	8.6
H	17.23	17.23	17.23

4.2 The Steam Density Coefficient

The reactivity change due to the uniform insertion of H_2O in the core of SNEAK 3 is caused primarily by additional moderation, partially also by reduced leakage. For the assembly 3 without fission products, the dependence of the multiplication constant k on the steam density in the coolant volume fraction of the core (35%) is shown in fig. 11. The normal hydrogen concentration in the coolant region of assembly 3 is chosen to correspond to that of a typical fast steam cooled power reactor, i.e., $\varrho_N = 0.07$ g/cm^3 /6/.

Of main interest is the range from $\varrho = 0$ (complete coolant loss) to $\varrho = 0.1$ g/cm^3. From a safety point of view, flooding of the reactor is considered a less serious problem than loss of coolant, since it will not occur as suddenly and can be controlled by some shut-down mechanism. The contributions to reactivity due to neutrons of energy E which are moderated to lower energies by collisions with hydrogen are shown in fig. 12 for three different steam densities. The net reactivity effect is the sum of large positive and negative contributions, and therefore it is hard to predict the change in the SDC caused by a small change in reactor composition. As soon as there are additional poisons such as Pu240 of fission products in the core, the SDC changes considerably; instead of an importance gain for degraded neutrons there may be a loss, and the multiplication factor k shown in fig. 11 does not reach such large values at high steam density /6/.

The neutron energy spectra and the importance spectra in the center of SNEAK 3 are shown for several steam densities in fig. 13 and 14. The hardening of the neutron spectrum due to coolant loss is abvious.

The experimental procedure of measuring the SDC appears difficult. Steam density changes throughout the entire core, blanket, or in zones of the reactor can be simulated

by varying the amount of polyethylene in the nickel tubes. This procedure is time consuming and, furthermore, the accuracy of such measurements depends upon the reproducibility associated with the loading procedure. Therefore only a few points on the curve $k(\varrho)$ will be measured. At the selected steam densities, also the slope $\frac{\Delta k(\varrho)}{\Delta \varrho}$ will be determined by material replacement measurements with the pile oscillator or sample changer. H_2O danger coefficients will be measured at certain steam densities at several locations in the core; the slope $\frac{\Delta k(\varrho)}{\Delta \varrho}$ for the entire core will then be found by spatial integration. Measurements at 3 or 4 steam densities in the region of main interest from $\varrho = 0$ to $\varrho = 0.1$ g/cm^3 should be sufficient.

The SDC experiments will be made inside the plutonium zone of assembly 3. SDC experiments at least 10 cm inside the boundary of the plutonium zone will yield information about an equivalent SDC experiment in an all-plutonium core with a test zone of equal size. It may then be feasible to extrapolate to the SDC of a plutonium core by gradually increasing the size of the test zone. Calculations have been made for 2 kinds of arrangements: 1) concentric spheres, and 2) sectors of increasing size.

In the concentric spheres experiment, the zone of maximum statistical weight (the center of the reactor) is used for the determination of moderation and absorption effects. The second experiment, using sectors, allows the measurement of leakage effects due to steam density changes. Reactivity effects caused by steam density changes in 1) concentric spheres of radius r_T inside a reactor with uranium driver, and 2) in an equivalent all-plutonium reactor are shown in table 6. Reactivity changes for corresponding experiments differ up to 20%, although statistical weights, fluxes, and adjoint fluxes in these zones agree within 2%. The difference is caused mainly by the moderation effect. The reactivity worth of neutrons of energy E which are moderated to the energy E' is proportional to $\phi(E)\left\{\phi^+(E')-\phi^+(E)\right\}$. The value $\phi^+(E')-\phi^+(E)$ is in the order of $\frac{1}{100}\phi^+(E)$ to $\frac{1}{10}\phi^+(E)$. A few percent deviation in ϕ^+ in the

Table 6: Spherical Zone Experiment in SNEAK 3

	All-Pu Core with Depl. U Blanket r_{core} = 53.2 cm	Pu Zone ($r \leq 39$ cm) with U Driver and Depl. U Blanket r_{core} = 53.2 cm
r_T = 53.2 cm	-1.47 +5.73	
r_T = 30 cm	-0.66 +2.71	-0.52 +2.39
r_T = 12 cm	-0.06 +0.27	-0.05 +0.24
r_T = 0.78 cm (calculated with perturbation theory)	$-2.08 \cdot 10^{-5}$ $+6.51 \cdot 10^{-5}$	$-1.77 \cdot 10^{-5}$ $+5.58 \cdot 10^{-5}$

Given in the above table is:

Percent change in k for steam density variations in a test zone of radius r_T.

Steam density change from $\varrho = 0.0735$ g/cm^3 to $\varrho = 0$
(upper left number)

from $\varrho = 0.0735$ g/cm^3 to $\varrho = 0.3$ g/cm^3
(lower right number)

U-Pu reactor relative to the all-plutonium reactor may account for the quite different moderation effects. The net reactivity effect, which is the sum of large positive and negative contributions of neutrons in the energy ranges 100 eV to 10 keV and 100 keV to 10 MeV, can easily differ by as much as 20%.

The sector experiments will be used to determine the radial dependence of the local SDC. It should also be possible to measure leakage effects accurately in a sector and to study the SDC due to steam density variations in the blanket. However, moderation differences between the U-Pu reactor and the all-plutonium reactor are more pronounced in this experiment.

The geometrical arrangement of the experiment is illustrated in fig. 15.

The multiplication constants for sectors of increasing size for the U-Pu reactor (curves B and C) and the all-plutonium reactor (curves A and D) with corresponding test zones are shown in fig. 16. Curves A and B give the reactivity change associated with an increase of steam density from ϱ_N to $\varrho = 0.3$ g/cm^3, curves C and D that for a change from ϱ_N to $\varrho = 0$.

The reactivity values for steam density changes in the all-plutonium core and/or the blanket can be determined with approximately 30% accuracy by simple extrapolation from sector experiments. By using more sophisticated extrapolation techniques, e.g., by correcting the statistical weight of the test zone for its deviations from linearity, the accuracy can be improved.

4.3 The Effect of Pu240 on the SDC

The effects of Pu240 on the SDC will be studied in a multizone version of SNEAK 3. A small test zone within the plutonium zone will be fueled with plutonium of the isotopic composition of interest. A search for the minimum allowable size

of the test zone was carried out at Karlsruhe by W.J. Oosterkamp using first order perturbation theory in connection with 26 group diffusion theory. The reactivity effects due to the oscillation of a polyethylene sample either in the test zone of the multizone reactor or in the same location of a reactor having the correct Pu240 content throughout were compared. Differences are caused by deviations of fluxes and adjoint fluxes in the two cases as well as by the different statistical weight of the perturbed region. Table 7 shows the error in the H_2O danger coefficients for three sizes of the test zone and for two Pu240 concentrations. The error caused by differences in statistical weight may be calculated rather accurately, thus reducing the total error.

It was concluded that about 5 kg of plutonium having a Pu240 isotopic content of 30% should be available in addition to the plutonium normally used. This amount will be sufficient to form a spherical zone of 135 mm radius (volume $\simeq$ 10 l), if a 30% Pu240 isotopic content is desired. Diluting this material in a 1:1 ratio with the standard SNEAK fuel will lead to a spherical zone of 170 mm radius (volume $\simeq$ 20 l) and a Pu240 content of 19%.

There will be an additional error introduced by the measurement technique. The polyethylene sample to be oscillated should be large enough to make the reactivity change easily detectable but not so large that it will severely perturb the flux spectrum. A cubic sample of 25 mm edge will produce a reactivity change of about $3 \cdot 10^{-6}$ Δk. If the precision of a pile oscillator measurement is $\pm 5 \cdot 10^{-8}$ Δk, such a measurement will have a relative error of about 2%. The estimated error of a danger coefficient measurement including both the epxerimental and systematic error due to spectral effects will amount to about 10% for a 135 mm zone of 30% Pu240 content, and to about 8% for a 170 mm zone of 19% Pu240 content.

Table 7: Error of Steam Danger Coefficient Evaluated at Normal Steam Density

	Atom Ratio Pu239/Pu240/Pu241/Pu242 80/17/2.5/0.5			63/30/5/2	
Radius of the Test Zone (mm)	60	120	180	60	120
Error due to Difference of Fluxes and Adjoint Fluxes (%)	23.0	9.2	5.0	20.6	-9.4
Error due to Differences of Statistical Weights (%)	1.8	1.9	2.1	6.7	-7.2

4.4 The Effect of Burn-up on the SDC

To study the effect of burn-up on the SDC in a fast steam-cooled reactor of medium size, experiments in assembly 3 are planned in which the core will be poisoned by fission products. It is foreseen that the plutonium zone will have a poison content which corresponds to an average burn-up of 23000 MWd/t using the fission product mock-up described in section 6.

4.5 The Effect of Heterogeneity on the SDC

Fig. 17 shows the calculated difference between k_{eff} values in homogeneous and heterogeneous cores at various steam densities. The curves are based on cell calculations for a geometrically simplified model of assembly 3 using cross sections from the 26 group ABN set. The main features of the calculational method are:

a) Collision probability methods are used to treat the transport problems.

b) Equivalence relations are used for heterogeneity corrections of self-shielded cross sections.

c) Heterogeneity corrections for the group diffusion constants are based on an approximate formula given by Benoist /7/.

Fig. 17 shows the large positive effects of heterogeneity at high water densities and the negative effect in the voided reactor.

Table 8 lists the components of the heterogeneity effect at various steam densities. The contribution due to changed diffusion constants, δk_D, is the dominant effect in the voided reactor, whereas for $\varrho_{H_2O} = 0.3$ g/cm^3 the greatest part of the heterogeneity effect can be interpreted as a change in the infinite multiplication factor k_∞.

Table 8: Heterogeneity Effects at Different Steam Densities

ϱ_{H_2O} (g/cm^3)	$\frac{\delta k_\infty}{k_\infty}$ (10^{-3})	δk_D *) (10^{-3})	$\frac{\delta k_{eff}}{k_{eff}}$ (10^{-3})
0	+2.6	-8.2	-5.6
0.0735	+6.2	-4.7	+1.5
0.3	+15.9	-2.2	+13.7

*) $k_D = \frac{\delta k_{eff}}{k_{eff}} - \frac{\delta k_\infty}{k_\infty}$

In a core without hydrogen, reactivity measurements on test zones with increased heterogeneity are planned. By performing such experiments with the test zones at different radial positions, we expect to be able to separate the effects of δk_D and δk_∞.

Similar experiments are planned in a core in which a steam density of approximately 0.3 g/cm^3 is simulated. In a central test zone of such a core, the δk_D component is negligible. Fine structure reaction rates will be measured with foils in order to test the calculated fine structure of the neutron flux in different energy regions.

5. Doppler Experiments

A broad program of Doppler measurements is planned for the SNEAK assemblies. These measurements will be directed not only toward the accurate experimental determination of temperature coefficients in typical fast reactor systems but also toward the verification of the adequacy of resonance cross sections and calculational techniques. In particular, the experimental approach is intended to be very flexible so that the temperature effects can be measured over a wide range of temperatures, sample volumes, sample compositions, and core compositions.

As a basis for the design of the experiments, a series of Doppler coefficient calculations has been carried out for SNEAK 2 and SNEAK 3. The primary goals of these calculations were, in addition to predicting the magnitude of the reactivity effects, 1) a study of the energy dependence of the Doppler effect, 2) a study of the Doppler coefficient as a function of coolant volume fraction or density, and 3) studies of the effectiveness of buffer zones surrounding the Doppler samples. The calculations were carried out using spherical reactor models, the 26 group ABN cross section set, diffusion theory, the Doppler program of Froelich /8/, and first order perturbation theory. Some of the results for the steam-cooled system are shown in figs. 18 and 19. The Doppler coefficient is approximately twice as large as for SNEAK 2; however, upon complete loss of coolant, the coefficient is reduced to less than one-third of its normal value. The studies also indicate that the coefficient's dependence upon coolant density may be experimentally determined by making the appropriate density changes in a small 15 liter volume at the center of the critical facility.

Figure 19 shows that, under normal conditions, the coefficient has a maximum at approximately 500 eV, and that the major part of the effect occurs between 100 eV and 1 keV, i.e., at energies considerably lower than in the sodium system. Therefore greater care must be taken to properly account for heterogeneity effects in the Doppler samples.

Two parallel experimental approaches are planned for the measurements in SNEAK:

1) Pile oscillator or auto-rod measurements with relatively small fuel samples (volume $\simeq$ 150 cm^3) heated electrically up to 1200°K.

2) A Doppler "Loop" in which hot gas is used to heat up, over a more limited temperature range, a center portion (as much as 4.5 liters) of the SNEAK assembly.

1. Oscillator Measurements: In this type of measurement, two essentially identical samples, one hot and one cold, are oscillated in and out of the reactor. Their reactivity differences is determined by application of either the pile oscillator or auto-rod techniques described in /9/. The samples are cylindrical in form, 15 cm long, and 3.5 cm in diameter. At present, four different sets of Doppler samples are planned: 1) $U^{238}O_2$-PuO_2 samples with various fractions of PuO_2; 2) UO_2 samples with various enrichment of U235; 3) $U^{235}O_2$-Al_2O_3 samples with $U^{235}O_2$ volume fractions ranging from 0.05 to 0.5; 4) PuO_2-Al_2O_3 samples with PuO_2 volume fractions ranging from 0.05 through 0.5. Samples of types 1) and 2) will cover ratios of fissile to fertile material which are plausible in fast reactor systems. It is hoped that Doppler measurements on types 3) and 4) will shed some light on the uncertainty surrounding the Doppler effect of fissile materials /10/, /11/. These latter samples will cover a broad range of σ_p (potential scattering per absorber atom) values, and therefore should provide an opportunity to study the adequacy of some of the calculation techniques used for lumped samples, e.g., the flat flux approximation and the sample-core interaction effect /12/.

2) Doppler Loop Measurements: The oscillator measurements described above, although having the advantage of covering a broad temperature range with high precision reactivity measurements, do not yield Doppler coefficients of the actual core composition. For this purpose, a test zone consisting of 1, 4, or 9 modified

SNEAK fuel elements can be inserted into the core and oscillated in temperature between 300 and 600°K. In contrast to the normal platelet construction of the SNEAK elements, the Doppler elements contain a quadratic 49 pin matrix with 0.6 cm diameter pins. These cladded pins are filled with the material necessary to achieve the desired overall test zone composition. Three basic pin compositions are planned: 1) $U^{238}O_2$ pins; 2) pins with mass of $U^{238}O_2$/mass of PuO_2 = 3; 3) pins containing structural materials or coolant simulants. The proper combination of types 1) and 2) can produce a test zone with fertile to fissile material ratios ranging from three to infinity. Sodium will be simulated by pins containing a lead-sodium alloy; the steam coolant will be simulated by pins containing zirconium hydride.

Doppler reactivity effects of the order 10^{-4} Δk are predicted for a ΔT of 300°K. Calculations using collision probability techniques have shown that the pin diameter is small enough to require only a small correction for heterogeneity effects.

6. Fission Product Mock-up

6.1 Introduction

The radiation level of many fission products prevents their use in a critical assembly. Therefore, a search was carried out for a mixture of stable elements which would simulate the reactivity effects due to the fission products. This mixture contains both fission product nuclides and mock-up materials.

In contrast to a former approach to this problem /13/, the energy dependent cross sections as given in /14/, /15/, and /16/ were used for calculating the composition of the mixture even though rather large uncertainties are associated with many of the cross sections. Our simulation procedure aims at minimizing that part of the effect considered (e.g., the reactivity change due to loss of coolant) that is contributed by mock-up materials.

Fission products with half lives of less than one year were replaced by their decay products, because the anticipated life of a fuel element will reasonably exceed one year. Secondary fission products, i.e.,nuclides that are produced by either neutron capture or radioactive decay of directly produced fission products, were taken into account. The total number of fission products considered amounts to 87.

6.2 Basis of Simulation

We introduce the following classification of fission products in order to simulate them by a mixture of stable elements (table 9).

The fission products in groups 1 and 5 do not necessitate any simulation. Those in group 2, producing more than half of the reactivity effect, have to be simulated in part only. The natural elements contain all fission products of this group, but their composition is not the one desired. This implies that the mock-up will contain some of the nuclides in this group in larger and some in smaller amounts than the original mixture. The nuclides which are not present in adequate amounts will be simulated by the surplus ones; the appropriate composition is determined using the cross section information.

All the fission products of groups 3 and 4 have to be simulated completely. It was aspired to substitute a fission product by a material whose absorption cross section has a similar energy behavior, at least with respect to the energy regions in which the main resonances occur. First order perturbation theory was used in the calculations, since the flux perturbation due to the exchange of a fission product with its substitute is rather small. All non-absorption effects were neglected. Replacing a certain fission product by its substitute may result in a small deviation of reactivity for the case of normal coolant density:

Table 9: Classification of Fission Products

The last column shows the relative contribution to the fission product effect on the loss of coolant reactivity.

Group	Characterized by Simulation: No	Partial	Total	Remarks	Fission Products Concerned	Relative Contribution (percent)
1	x			Elements with only one stable isotope	Rh103, I127, Cs133 La139, Pr141	15.5
2		x		Isotopes of elements with more than one stable isotope	All that are stable isotopes of Zr, Mo, Ru, Pd, Ag, Cd, Ce, Nd, Sm, Eu, Gd	54.5
3			x	Gaseous at room temperature	Kr85, all isotopes of Xe	3.5
4			x	Radioactive	Zr93, Tc99, Pd107, I129, Cs135, Pm147, Sm151, Eu154, Eu155	26.0
5	x			Contribute too little to be considered	Se82, Kr83, Kr84, Kr86, Rb85, Rb87, Sr88, Sr90, Y89, In115, Te126, Te128, Te130, Cs137, Ba134, Ba136, Ba137, Ba138, Tb159	0.5

$$k_1 = \frac{\int\left[\Sigma_a^o(E)-\Sigma_a^s(E)\right]\phi_1(E)\phi_1^*(E)dE}{\int\chi_1(E')\phi_1^*(E')\int\nu(E)\Sigma_f(E)\phi_1(E)dE'dE}$$

where $\Sigma_a^o(E)$ = macroscopic absorption cross section of the fission product

$\Sigma_a^s(E)$ = macroscopic absorption cross section of the substitute

subscripts 1 and 2 refer to normal and zero coolant density, respectively, and all the other symbols have their usual meanings.

Another deviation may result if the same replacement is done at zero coolant density. If we require that these two deviations be equal ($\Delta k_1 = \Delta k_2$) we obtain the correct reactivity change for loss of coolant. This leads to the expression

$$\frac{\int\Sigma_a^o(E)\phi_1(E)\phi_1^*(E)dE}{\int\chi_1(E')\phi_1^*(E')\int\nu(E)\Sigma_f(E)\phi_1(E)dEdE'} - \frac{\int\Sigma_a^o(E)\phi_2(E)\phi_2^*(E)dE}{\int\chi_2(E')\phi_2^*(E')\int\nu(E)\Sigma_f(E)\phi_2(E)dEdE'} = \frac{\int\Sigma_a^s(E)\phi_1(E)\phi_1^*(E)dE}{\int\chi_1(E')\phi_1^*(E')\int\nu(E)\Sigma_f(E)\phi_1(E)dEdE'} - \frac{\int\Sigma_a^s(E)\phi_2(E)\phi_2^*(E)dE}{\int\chi_2(E')\phi_2^*(E')\int\nu(E)\Sigma_f(E)\phi_2(E)dEdE'}$$

This equation can be satisfied by multiplying each $\Sigma_a^s(E)$ by a constant factor, i.e, by adjusting the amount of the simulating material.

6.3 Estimation of Error

It was examined what part of the reactivity effect is due to the correct fission product nuclides present in the correct amounts. In order to do so, the reactivity contribution of each fission product nuclide was calculated. This value then was compared to the reactivity contribution of the same nuclide of the mock-up. The smaller of the two values was termed the correct reactivity contribution. It can be shown that this method is in

favor of simulating the fission products in group 3 and 4 by elements of group 2.

One may also use this method to find the "best" composition of different elements simulating those fission products they contain as isotopes. It is usually of advantage to determine in one calculation the simulating mixture for isotopes that belong to two or three elements. By variation of the amounts to be used of each element, the simulation error may be decreased.

The reactivity contributions were calculated by first order perturbation theory. Though some of the fission products will produce a non-negligible flux perturbation if added to the reactor, this method appears to be sufficient for an error analysis.

A similar comparison as done for the reactivity contributions was performed for the mass contributions.

6.4 Application

Table 10 shows the composition of the mock-up simulating the fission products for a typical steam-cooled fast reactor of 300 MW thermal power for an anverage burn-up of about 23000 MWd/t. The isotopic quantity of the elements krypton, xenon, and cesium was reduced by 50% to account for their escape from the core.

Table 10: Composition of the Mock-up

Material	Amount (kg)	Material	Amount (kg)
Molybdenum	10.405	Cesium	1.294
Ruthenium	5.750	Lanthanum	2.302
Rhodium	1.663	Cerium	4.761
Palladium	4.680	Praseodymium	2.144
Silver	1.608	Neodymium	8.146
Cadmium	0.212	Samarium	3.338
Iodine	0.371	Europium	0.290
		Gadolinium	0.138

Note: Rhodium, palladium, and ruthenium, which are rather expensive, will partly be substituted by other materials on an experimental basis.

The reactivity effect due to fission product nuclides present in the correct quantity amounts to 58.3% of the fission product-induced reactivity change due to loss of coolant. The error introduced by simulating a certain nuclide by a different one was estimated to amount to between 30 and 40%. This will result in a 13 to 17% total uncertainty in the reactivity change due to loss of coolant. In the mixture, 57.5 $^{w}/_{o}$ is contributed by fission products present in the correct amounts.

In practice most of the materials will be used in the form of oxides with the exception of rhodium, ruthenium, palladium, silver, and cadmium which will be present as metals, and iodide and cesium which will be used in the form of AgI and Cs_2CO_3.

Because of lack of space, all zirconium fission products were simulated by molybdenum. This does not change the simulation error notably.

6.5 Versatility of the Mock-up

The fission product mock-up was calculated to give best agreement for the fission product contribution to the reactivity change due to loss of coolant in a steam-cooled reactor. The effect this particular mock-up would have for other conditions is shown in table 11. It gives the systematic deviation (in percent of the correct value) one would obtain by using the mock-up that was calculated for coolant loss of a steam-cooled reactor for other situations. The results imply that the mock-up is much more versatile than one might have expected.

All calculations were done by means of a FORTRAN program written for an IBM 7074 computer. The fission yields were taken from /17/. The spectra and importance spectra were obtained by a 26 group diffusion theory calculation. A more detailed treatment of the fission product mock-up will be published elsewhere.

Table 11: Versatility of the Mock-up

Effect of Interest: Reactivity Change Due to	Reactor Type	% Systematic Deviation in δk
Coolant loss	steam-cooled	0 (reference)
Coolant loss	steam-cooled softer spectrum *)	+5
Accumulation of fission products **)	steam-cooled	-4
Coolant loss	sodium-cooled	-8
Accumulation of fission products **)	sodium-cooled	-6

*) Flux below 2 keV artificially increased by factors up to 10 in the lowest groups

**) Average burn-up 23000 MWd/t

References:

/1/ A.G. EDWARDS: A Zoned Loading for a ZPR-3 Facility, ANL-6927

/2/ T.C. ENGELDER et al.: Accuracy of Power Reactor Void Coefficients Extrapolated from Measurements in Critical Assemblies, ANL-7120, p. 585-597

/3/ R. DURAND-SMET: Zur Frage der Bestimmung neutronenphysikalischer Größen von Natrium-gekühlten Schnellen Brutreaktoren mit der SNEAK-2-Anordnung, KFK-382

/4/ L.P. ABAGJAN et al.: Gruppenkosntanten schneller und intermediärer Neutronen für die Berechnung von Kernreaktoren, KFK-tr-144

/5/ H. KÜSTERS and M. METZENROTH: The Influence of Some Important Group Constants on Integral Fast Reactor Quantities, ANL-7120, p. 423-433

/6/ E. KIEFHABER and K. OTT: Survey Parameter Study of Large Steam-Cooled Fast Power Reactors, ANL-7120, p. 815-825

/7/ P. BENOIST: Theorie du coefficient de diffusion des neutrons dans un réseau comportant des cavitées, CEA-R-2278

/8/ R. FROELICH and K. OTT: About the Influence of Resonance Overlapping on Calculated Doppler-Coefficients of Fast Reactors, Nucl.Sci.Eng. 22, p. 490-492

/9/ P. ENGELMANN et al.: Construction and Experimental Equipment of the Karlsruhe Fast Critical Facility, SNEAK, KFK-471

/10/ G.J. FISCHER et al.: Measurement and Analysis of Doppler Effect in Plutonium-fueled Fast Reactor Assemblies, ANL-7120, p.603-609

/11/ A.R. BAKER and R.C. WHEELER: Doppler Coefficient Measurements in Zebra Core 5, ANL-7120, p. 553-565

/12/ E.A. FISCHER: Interpretation of Doppler Coefficient Measurements in Fast Critical Assemblies, KFK-473

/13/ D. OKRENT: The Sensitivity of Breeding Ratio in Fast Reactors to Uncertainties in Cross Sections, ANL-6122, p. 93-100

/14/ G.D. JOANOU et al.: Nuclear Data for GAM-1 Data Tape, GA-2451

/15/ J.D. GARRISON and B.W. ROOS: Fission Product Capture Cross Sections, Nucl.Sci.Eng. 12, p. 115-134

/16/ R.C. LIIKALA: Updated R.B.U. Basic Library, HW-75716

/17/ I.F. CROALL and H.H. WILLIS: Some Yields in the Thermal- and Epi-Cadmium-Neutron Fission of Pu239, Proc. of the IAEA Symposium on Physics and Chemistry of Fission, Vol. 1, p. 355 (1965)

Fig. 1 Sector Experiments in All-Plutonium Core

Neutron Flux at r = 41.2 cm as a function of the angular ordinate Θ when sectors of different magnitude are voided of Sodium.

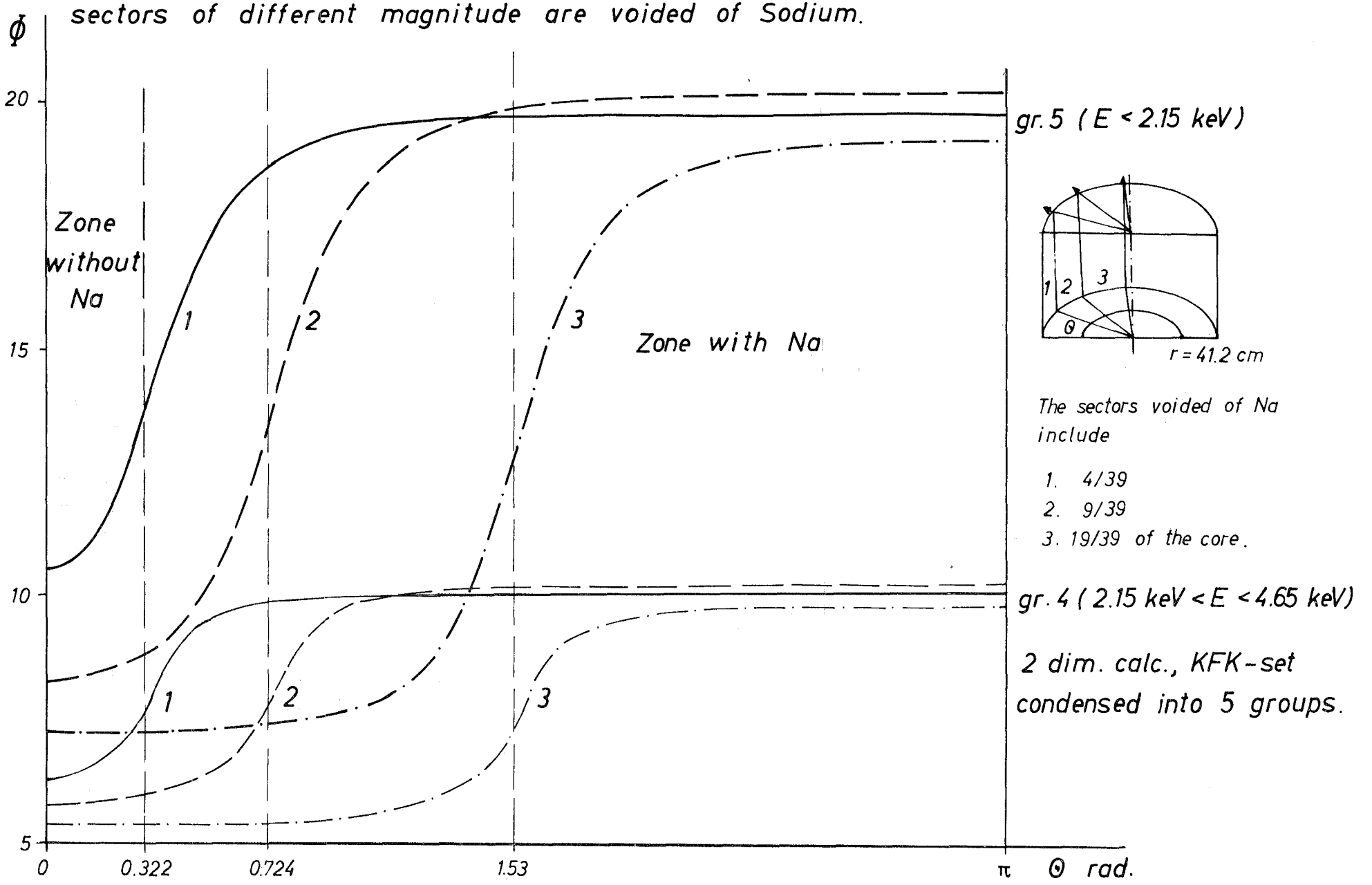

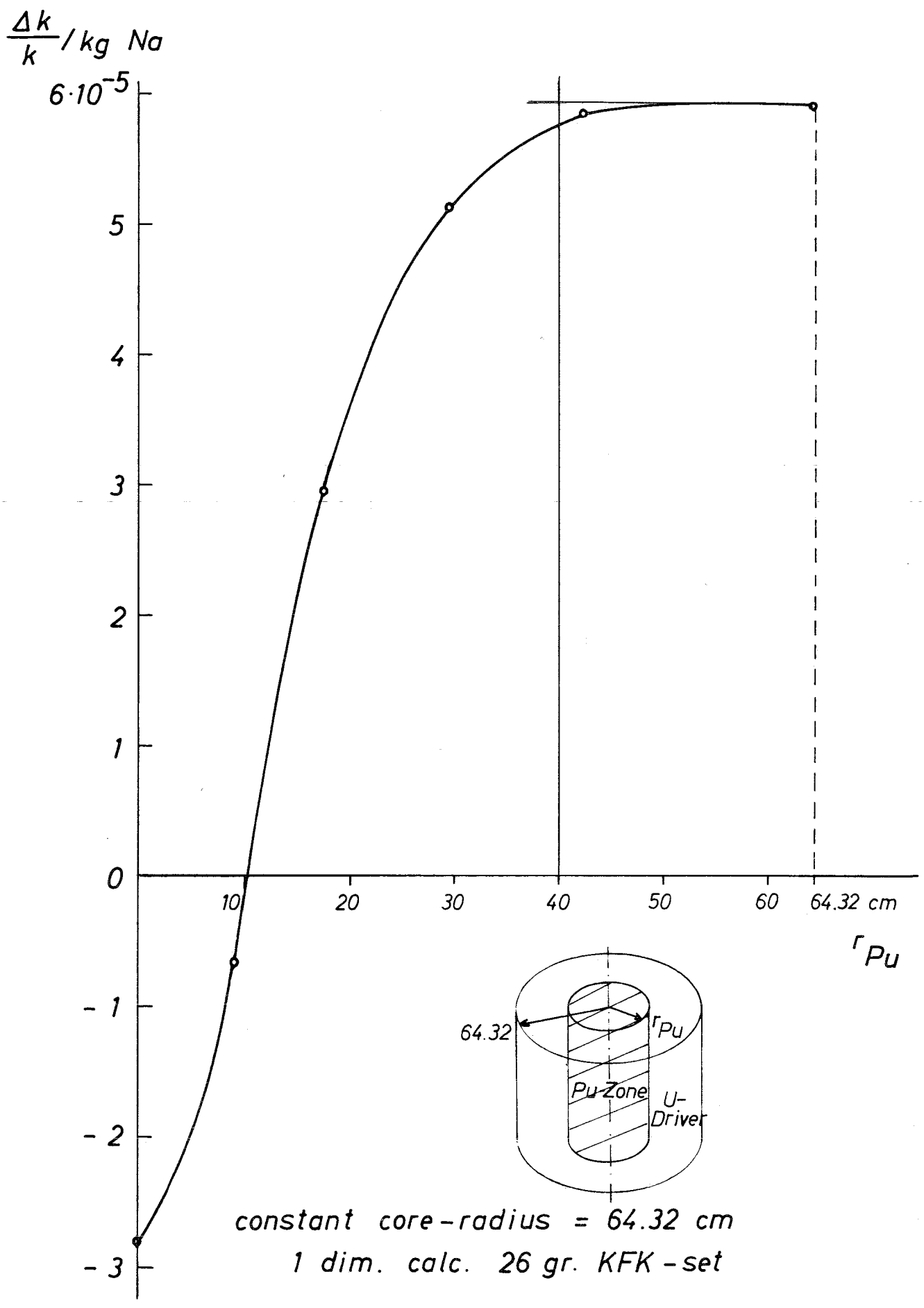

Fig. 2 Mean Sodium Danger Coefficient at the Core Axis as a Function of the Radius of the Plutonium Zone

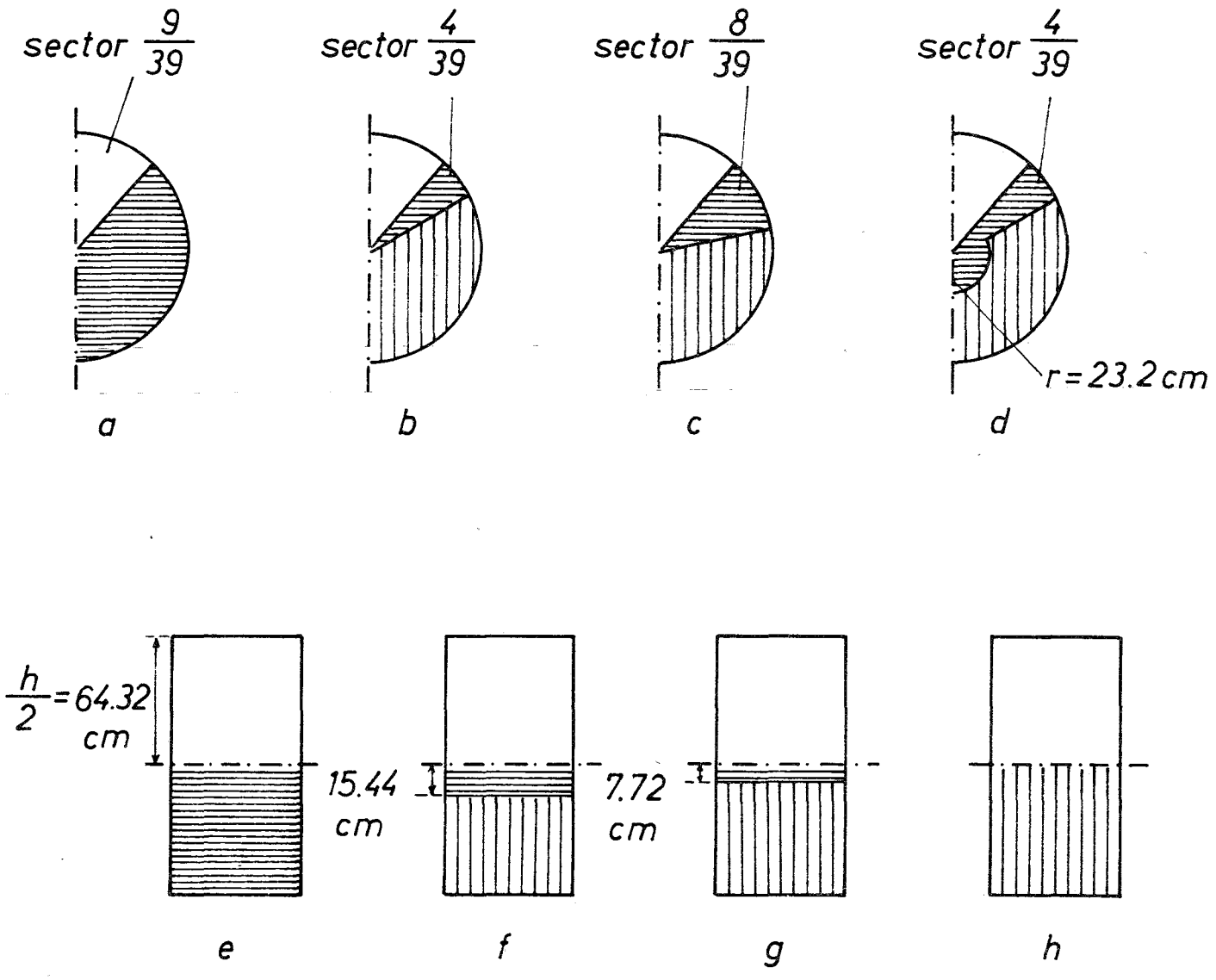

Fig. 3 Configurations to Study the Influence of the Uranium Driver

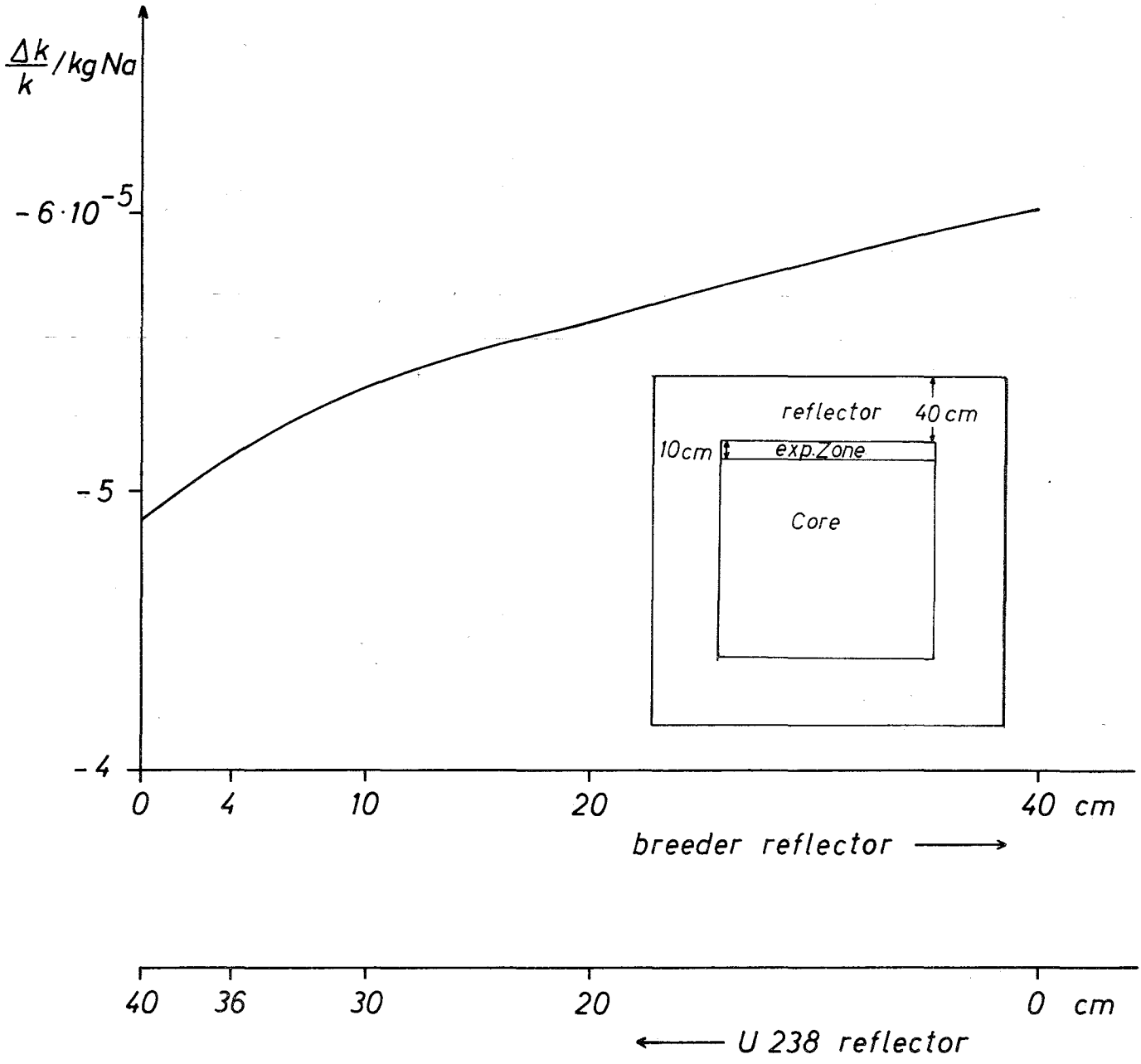

Fig. 4 Influence of Axial Reflector Composition on Sodium Coefficient

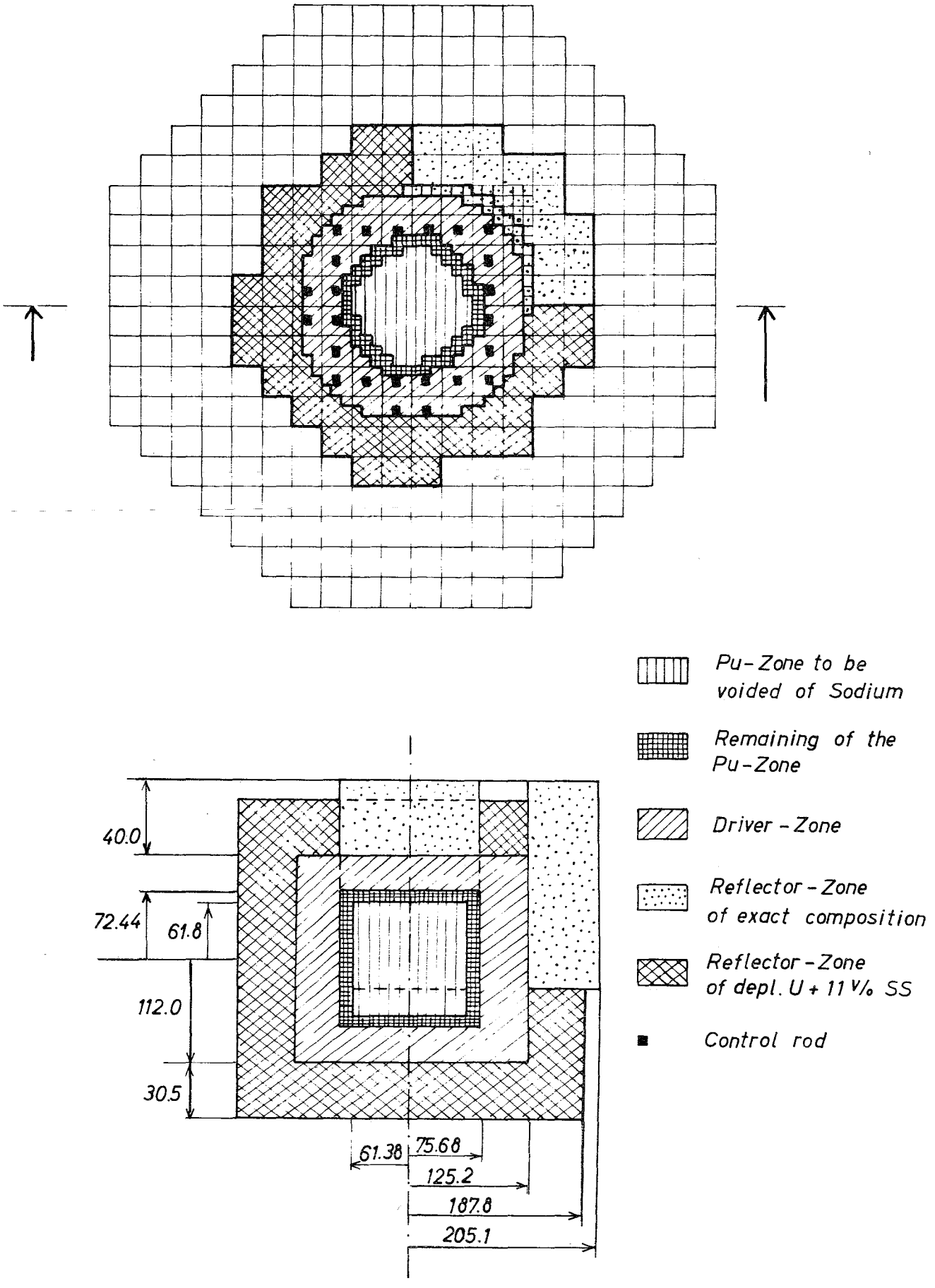

Fig. 5 Horizontal and Vertical Section through Assembly SNEAK 2

Configuration for Central and Axial Experiments

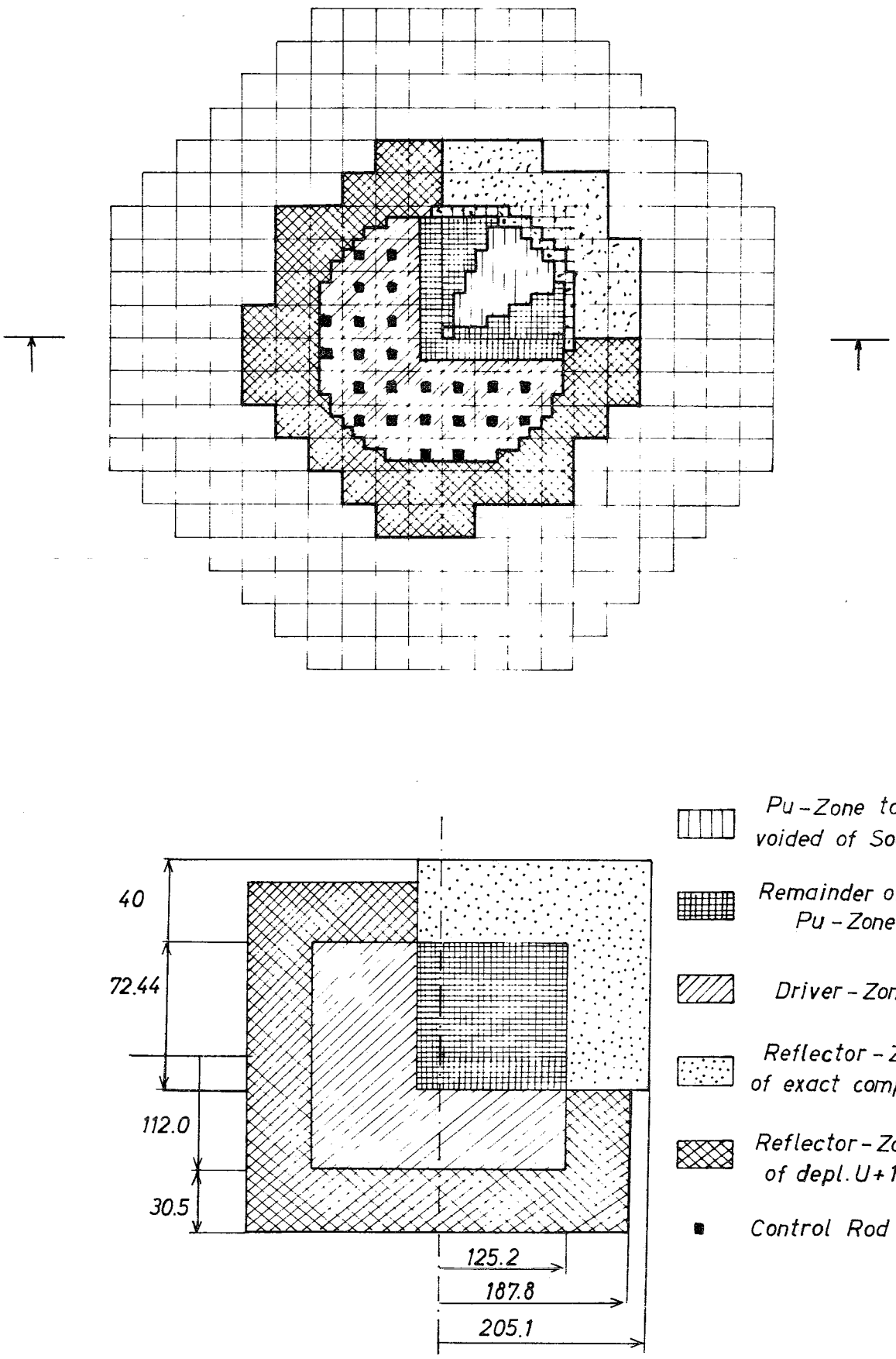

Fig. 6 Horizontal and Vertical Section through Assembly SNEAK 2

Configuration for Sodium Void Experiments in an Angular Core Sector

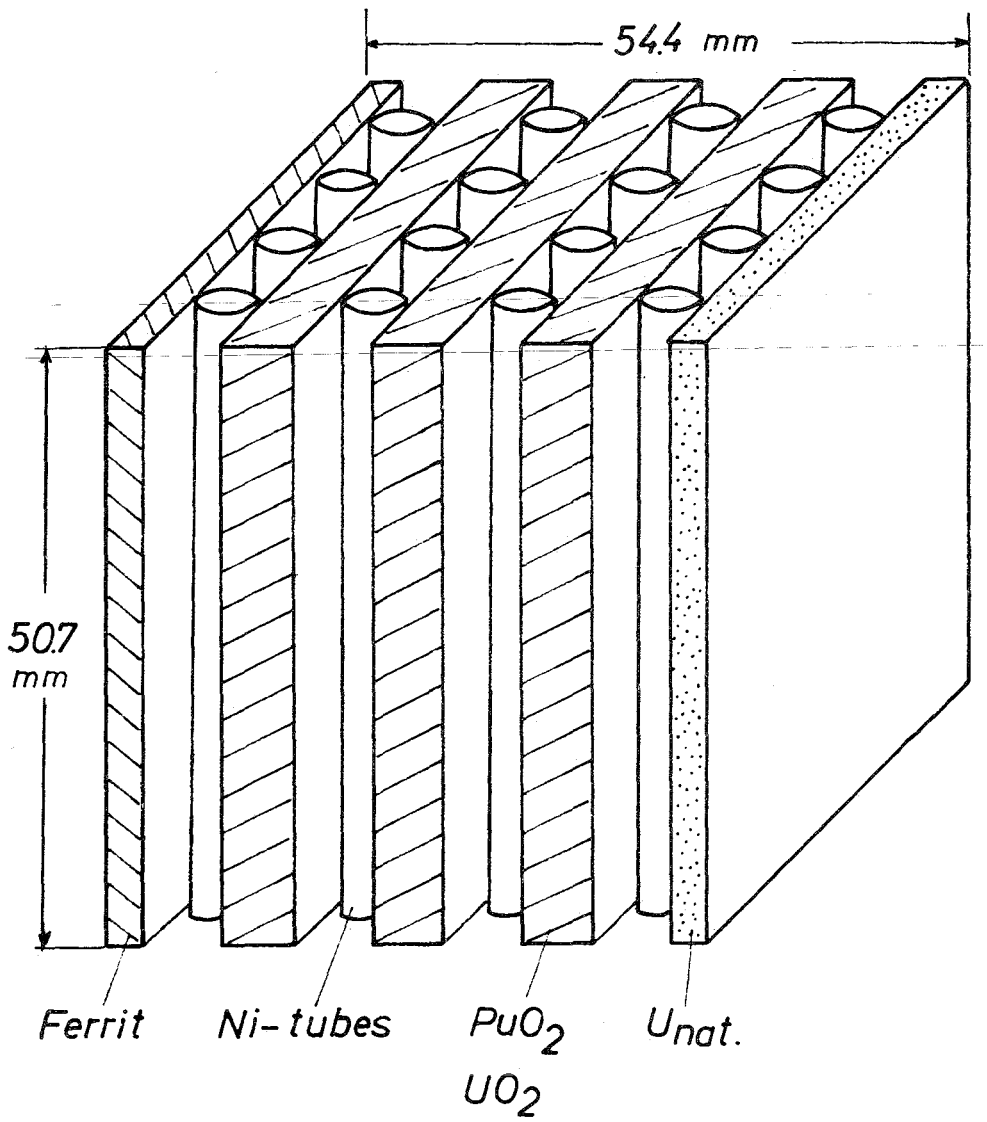

Fig. 7 Unit Cell of SNEAK 3

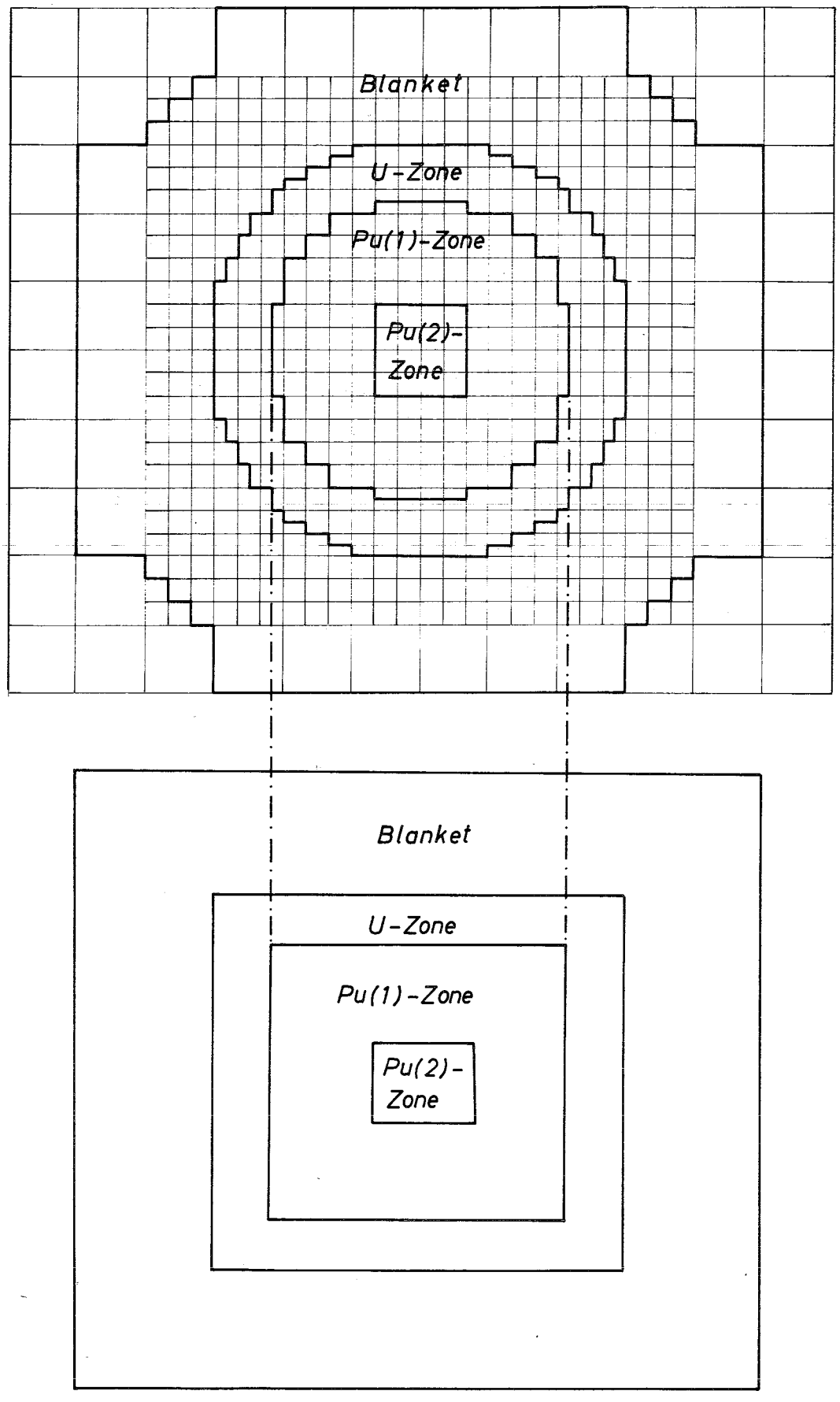

Fig. 8 Horizontal and Vertical Section through Assembly SNEAK 3

Volume of the plutonium-zone 268 l, enrichment 1/7

Volume of the uranium-zone 445 l, enrichment 1/5

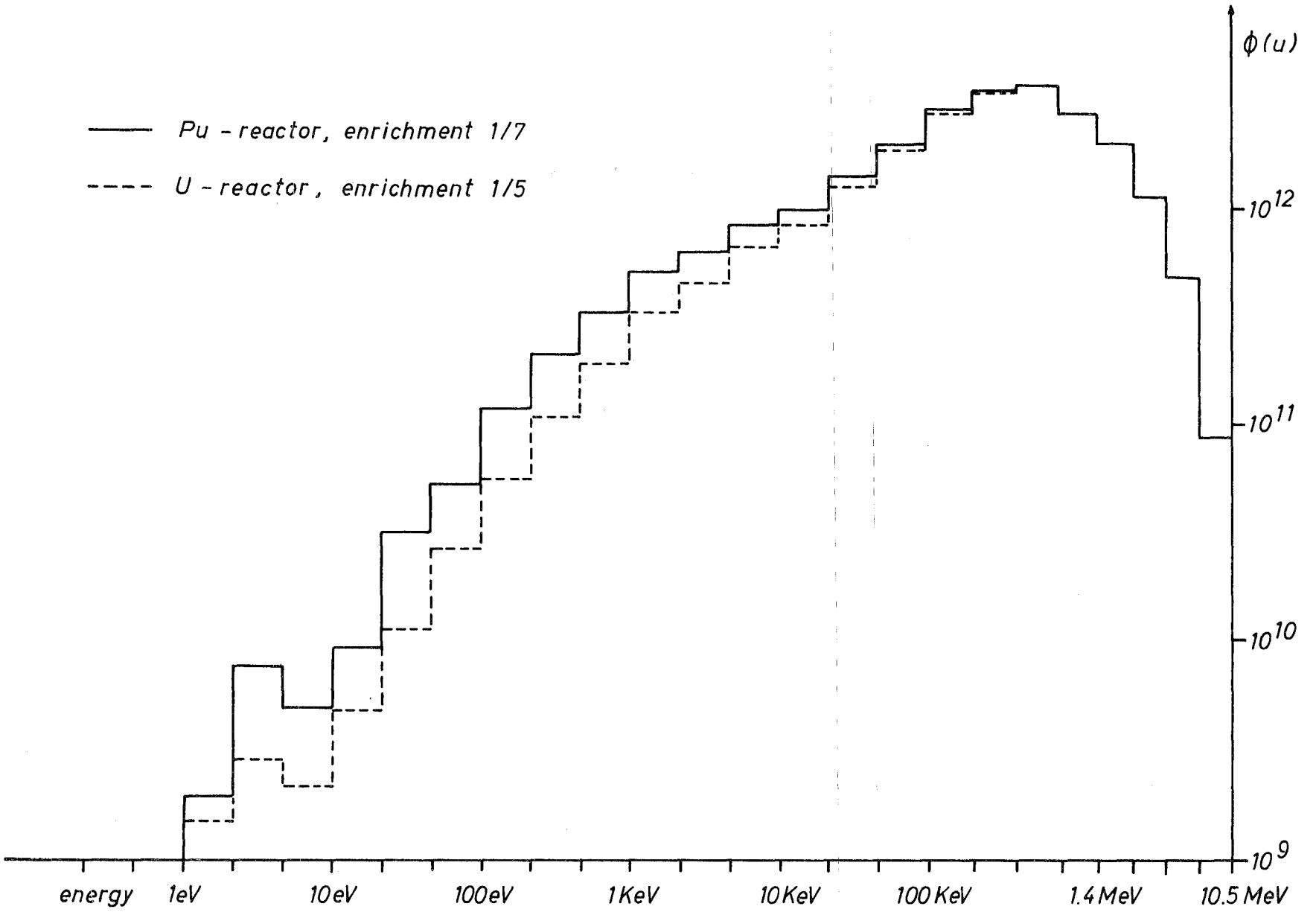

Fig. 9 Comparison of Neutron Energy Spectra (Flux per Unit Lethargy)

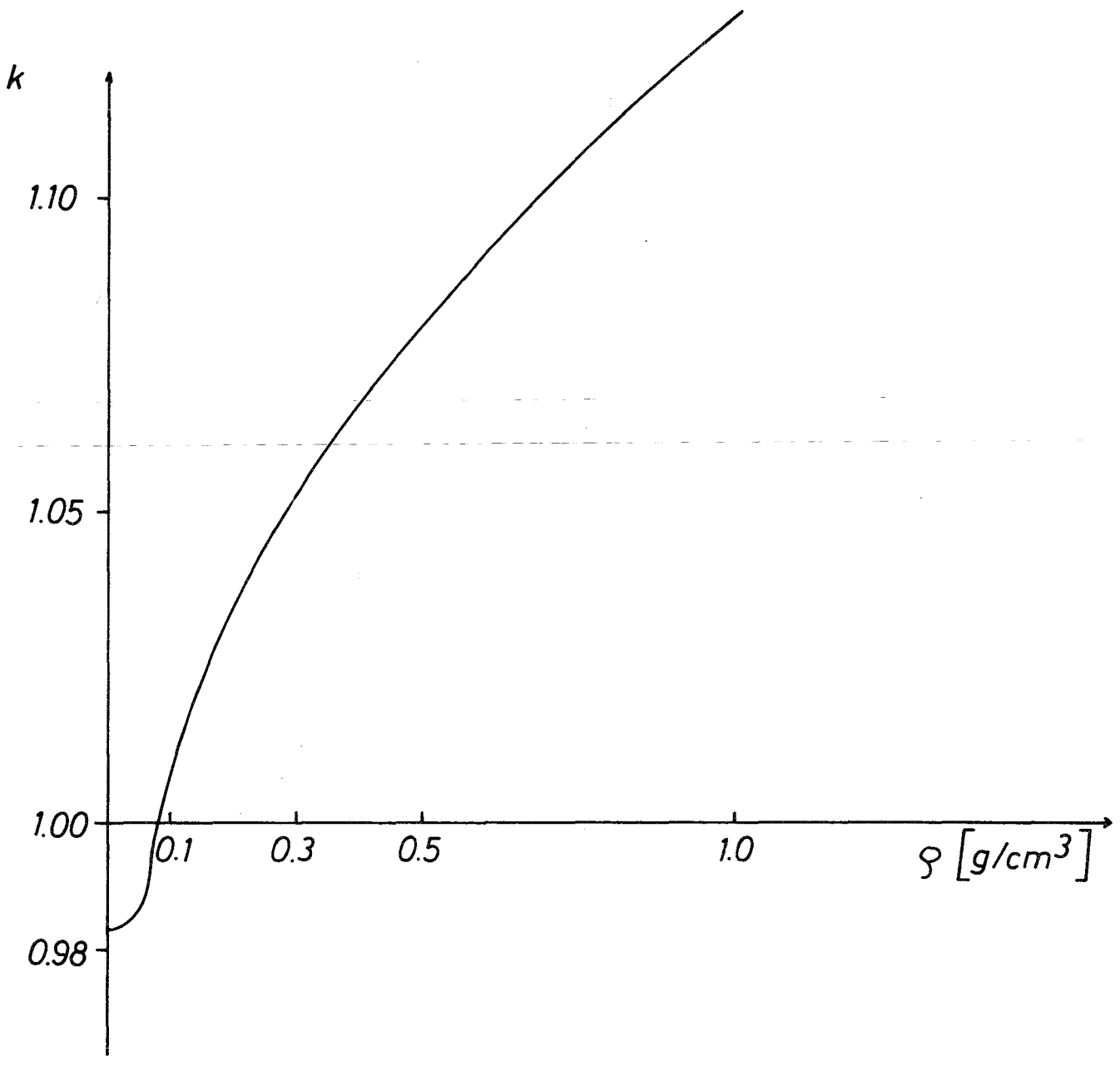

Fig. 11 Dependence of Multiplication Factor on Steam Density in Assembly 3 (Without Fission Products)

Spherical Core with 53.2 cm Radius and Depleted Uranium Blanket

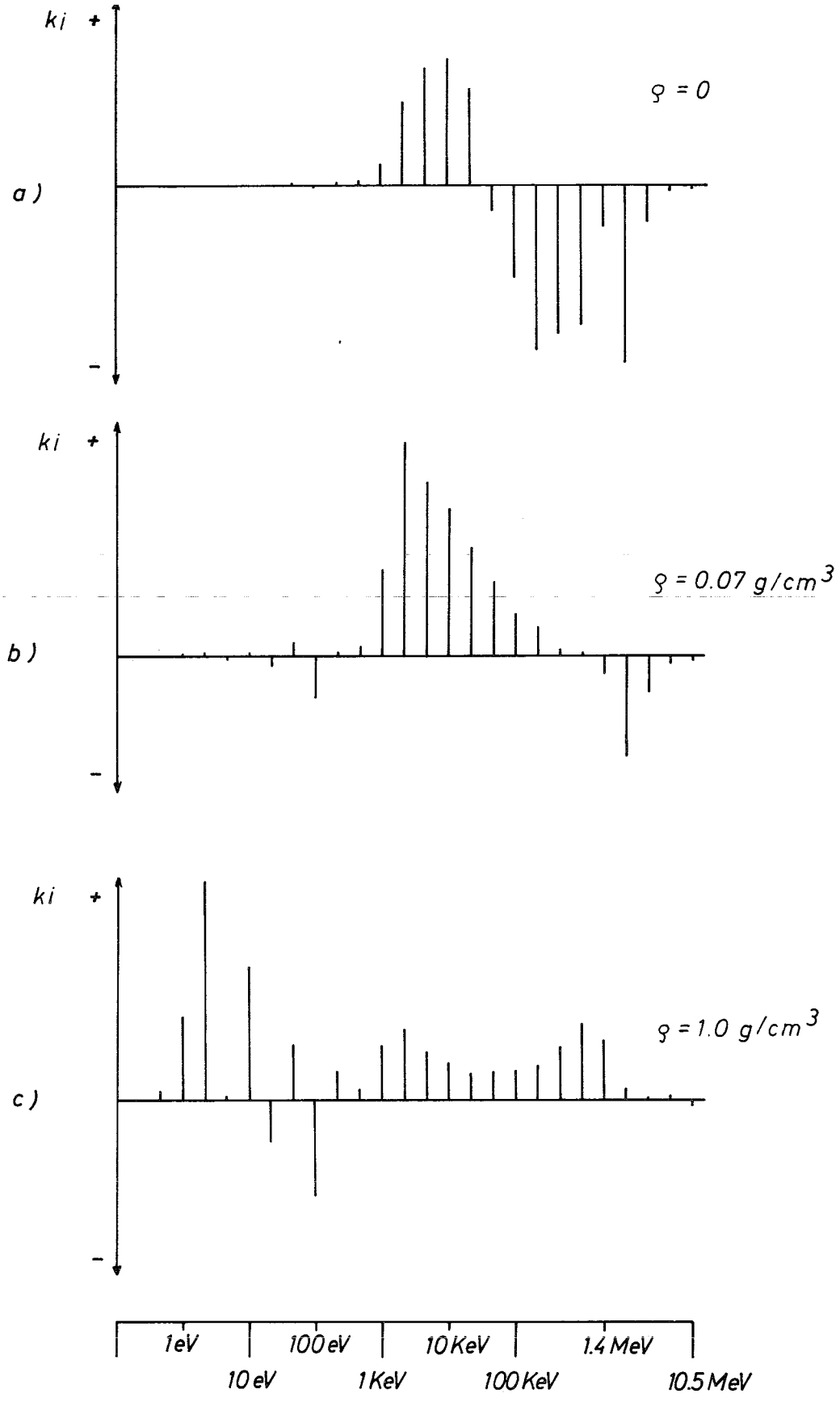

Fig. 12 Relative Contributions of Flux Moderation to the SDC

$$k_i \sim \sum_j \sigma_{i \to j} \, \phi_i \, (\phi_j^+ - \phi_i^+)$$ (i=Energy Group Number)

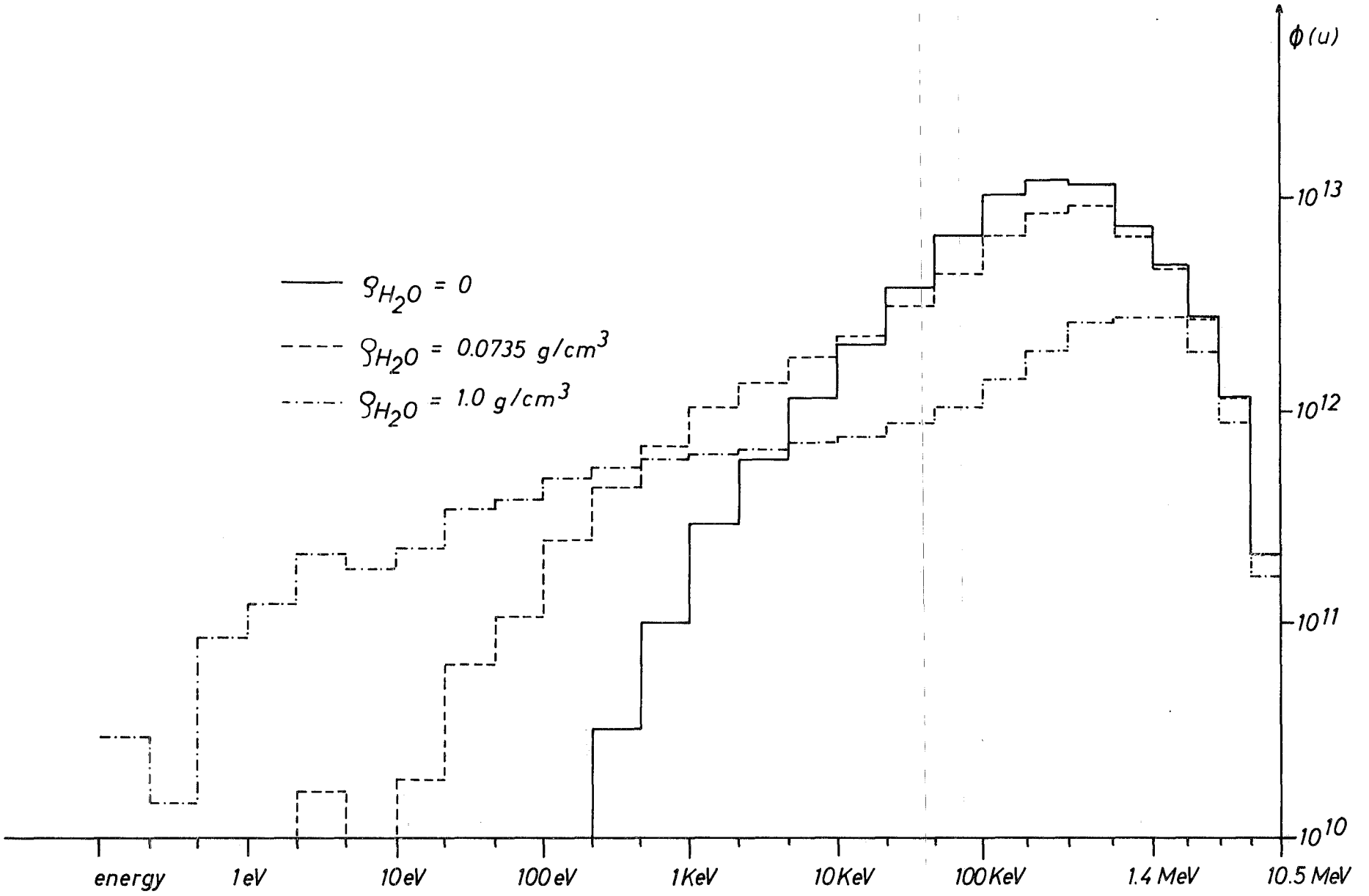

Fig. 13 Neutron Spectrum at the Center of Assembly 3 at Three Different Steam Densities (Without Fission Products)

Flux per Unit Lethargy

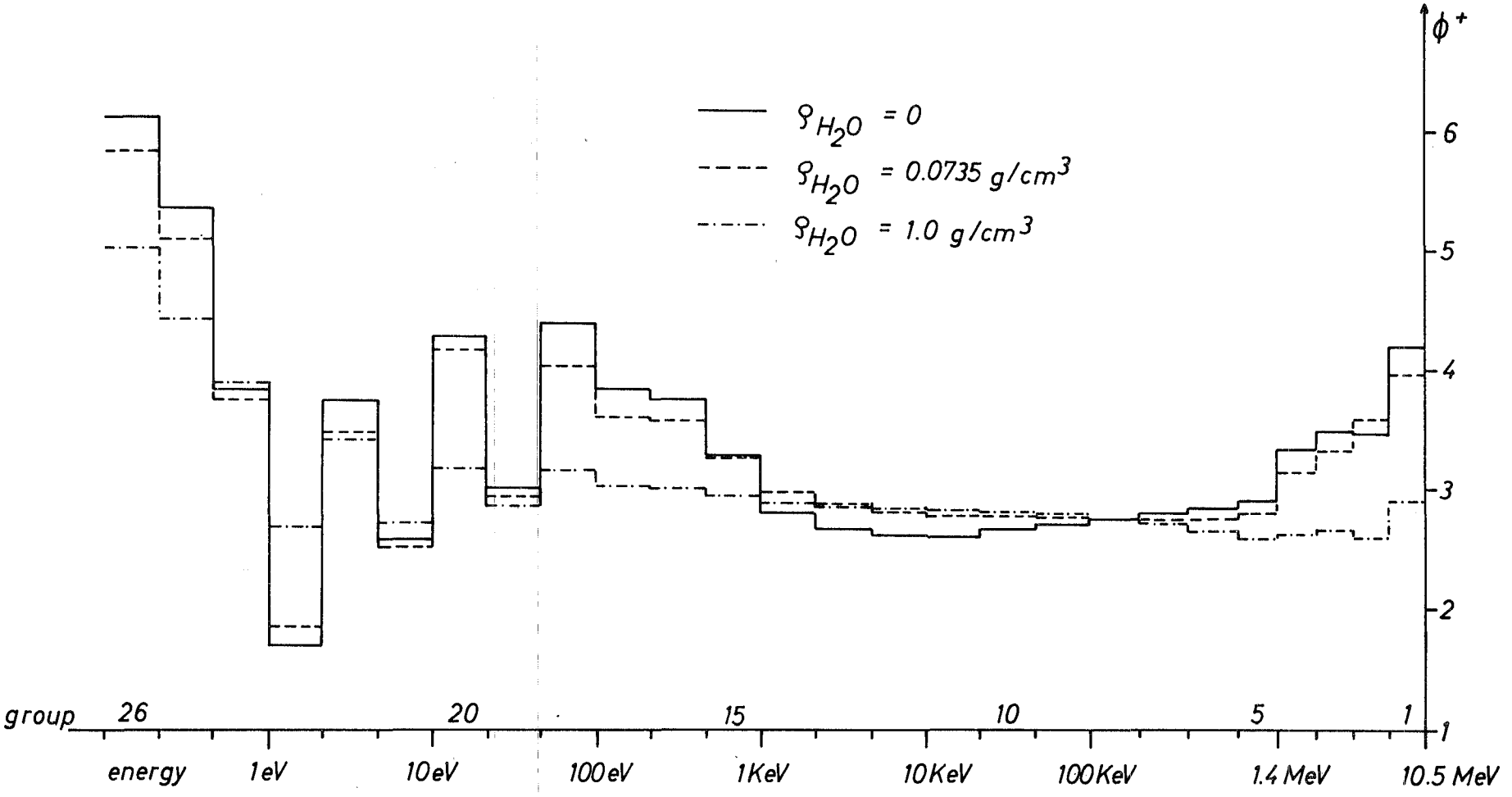

Fig. 14 Adjoint Spectrum at the Center of Assembly 3 at Three Different Steam Densities (Without Fission Products)

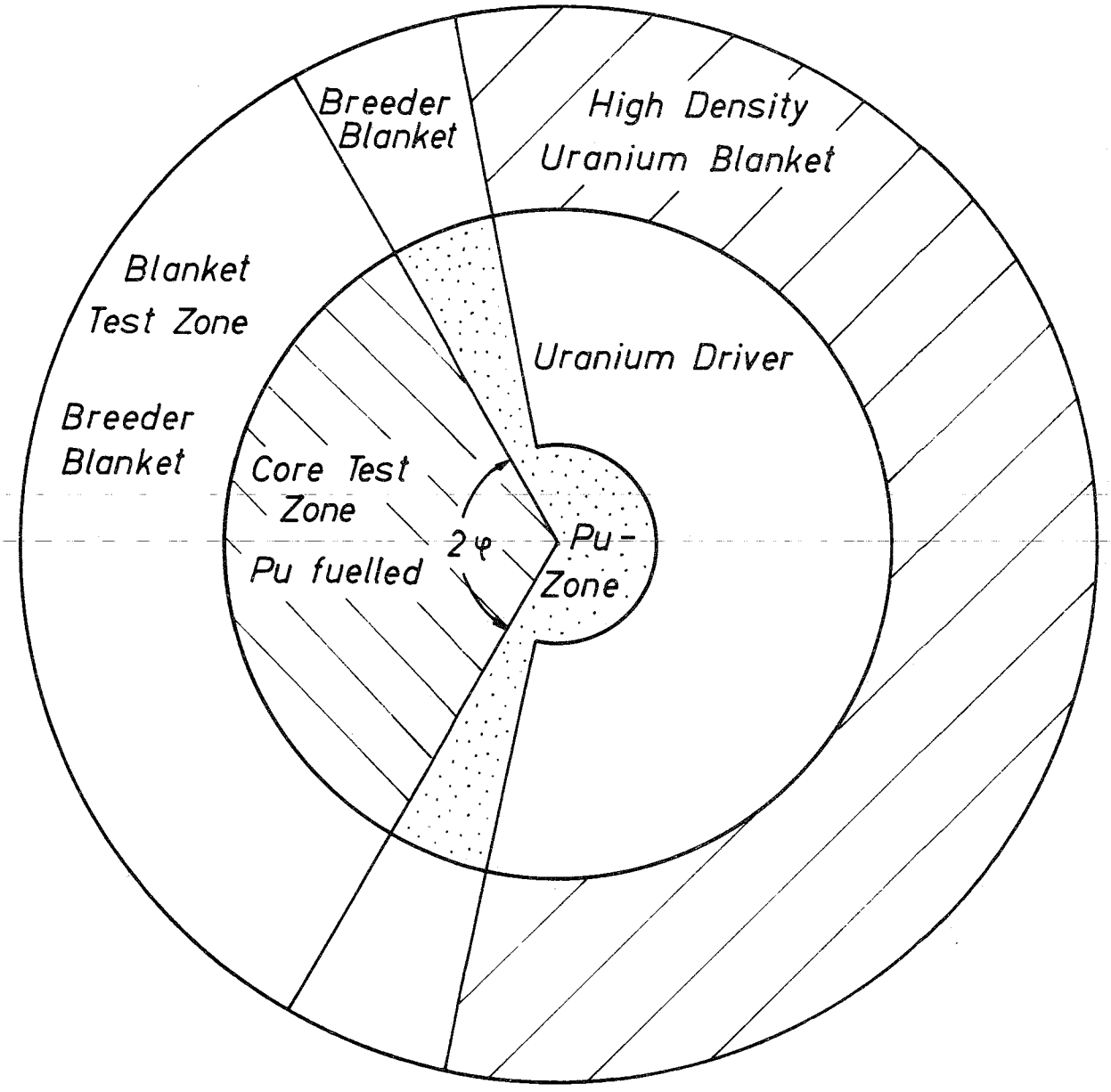

Fig. 15 Arrangment for SDC Sector Experiments in Assembly 3

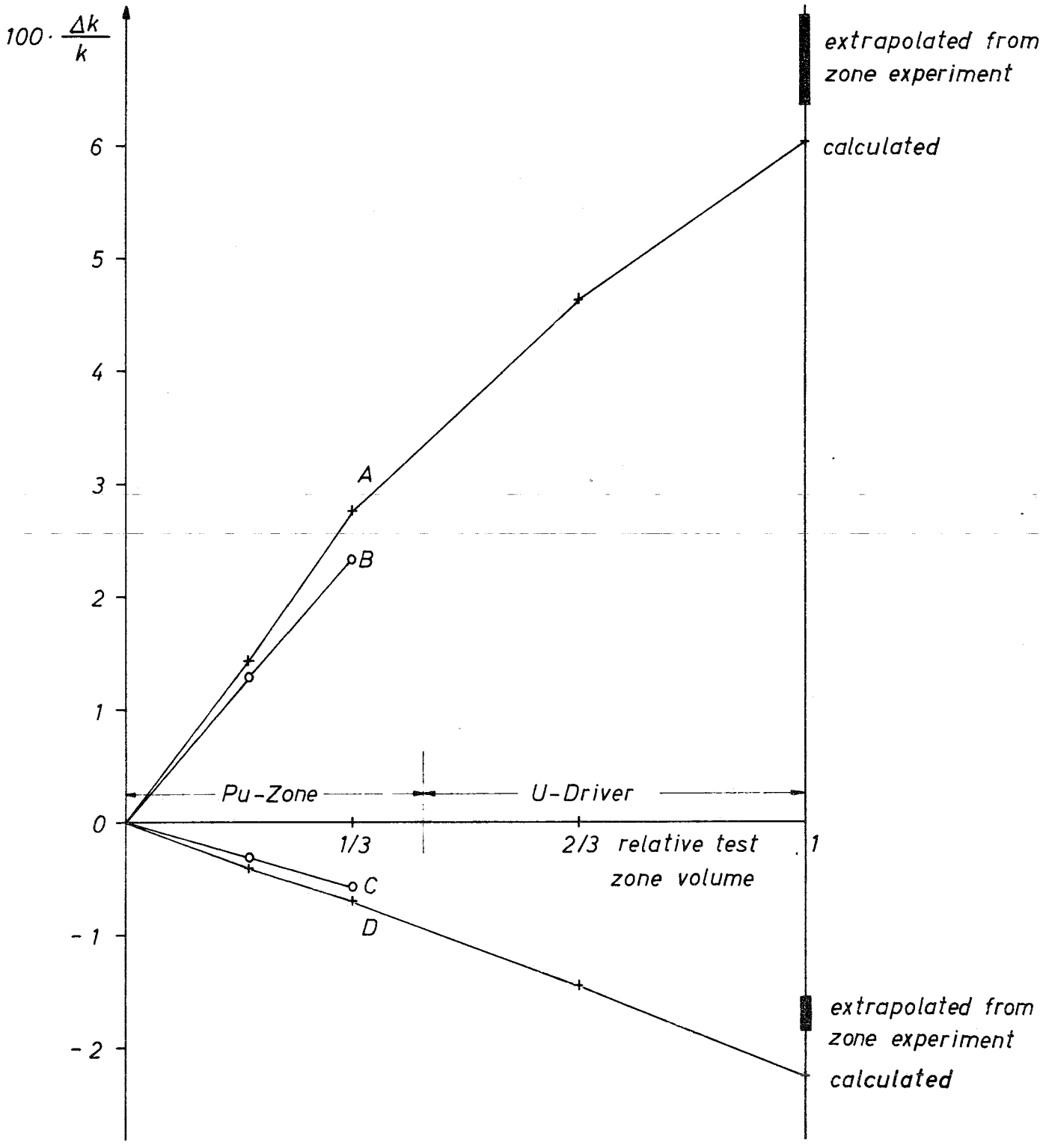

Fig. 16 Calculated Reactivity Changes for Sector Experiments

Curves A, C : all-Pu-reactor ; B, D : U-Pu-reactor

A, B : steam density change in the test zone from ϱ = 0.07 g/cm^3 to ϱ = 0.3 g/cm^3

C, D : steam density change in the test zone from ϱ = 0.07 g/cm^3 to ϱ = 0

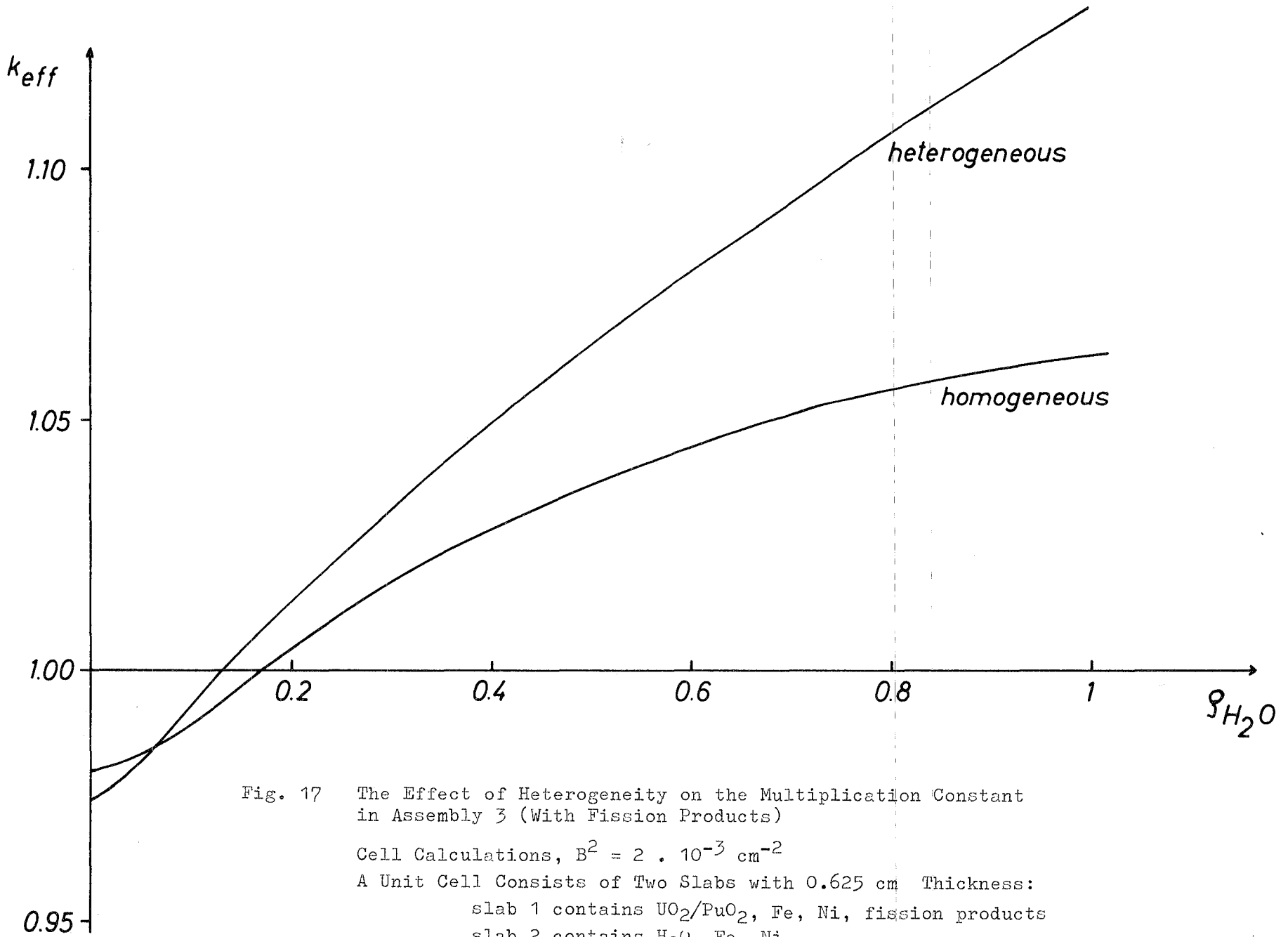

Fig. 17 The Effect of Heterogeneity on the Multiplication Constant in Assembly 3 (With Fission Products)

Cell Calculations, $B^2 = 2 \cdot 10^{-3}$ cm^{-2}

A Unit Cell Consists of Two Slabs with 0.625 cm Thickness:

slab 1 contains UO_2/PuO_2, Fe, Ni, fission products

slab 2 contains H_2O, Fe, Ni

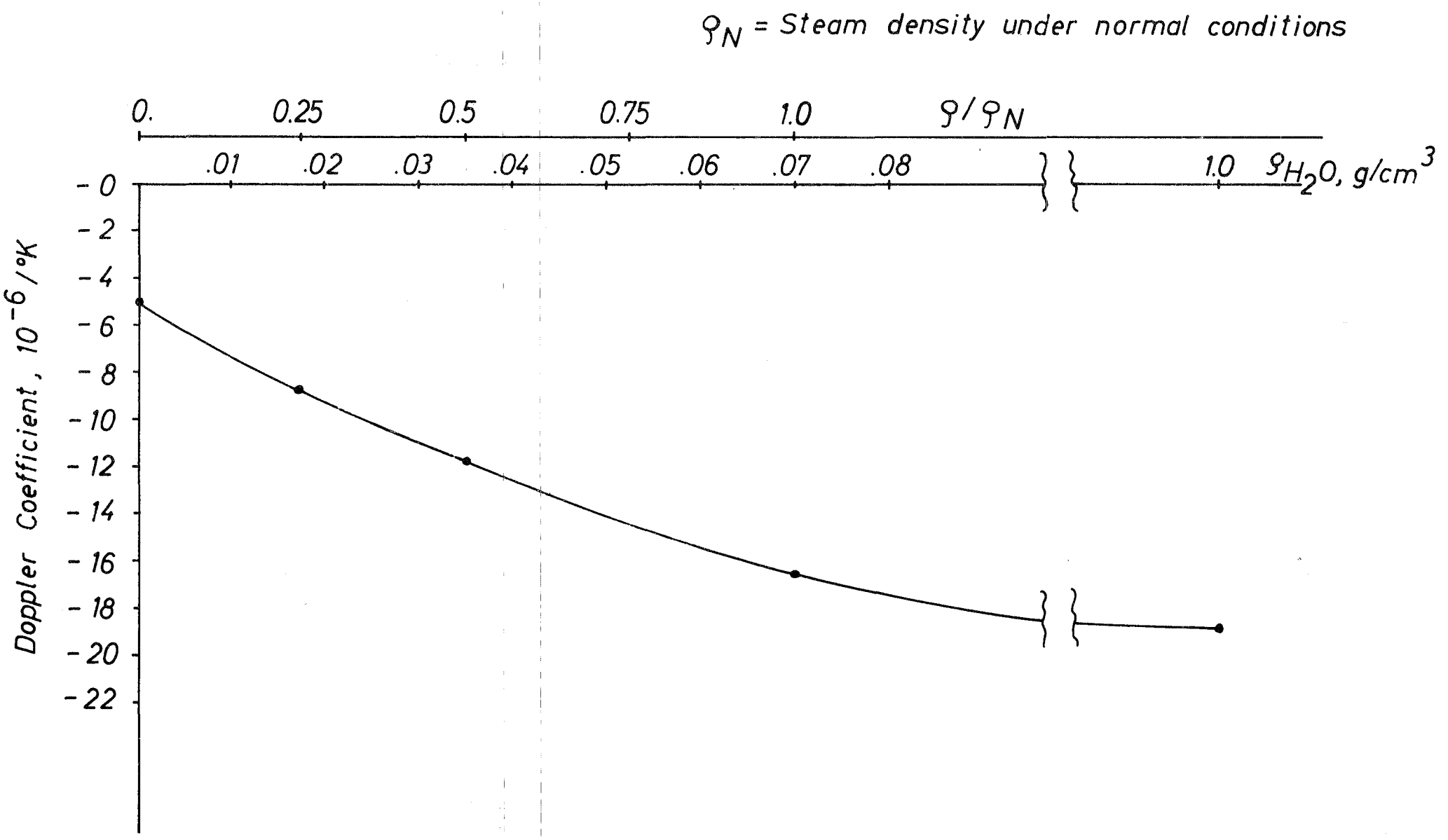

Fig. 18 Total Doppler Coefficient of the SNEAK 3 Plutonium Reactor at 900°K

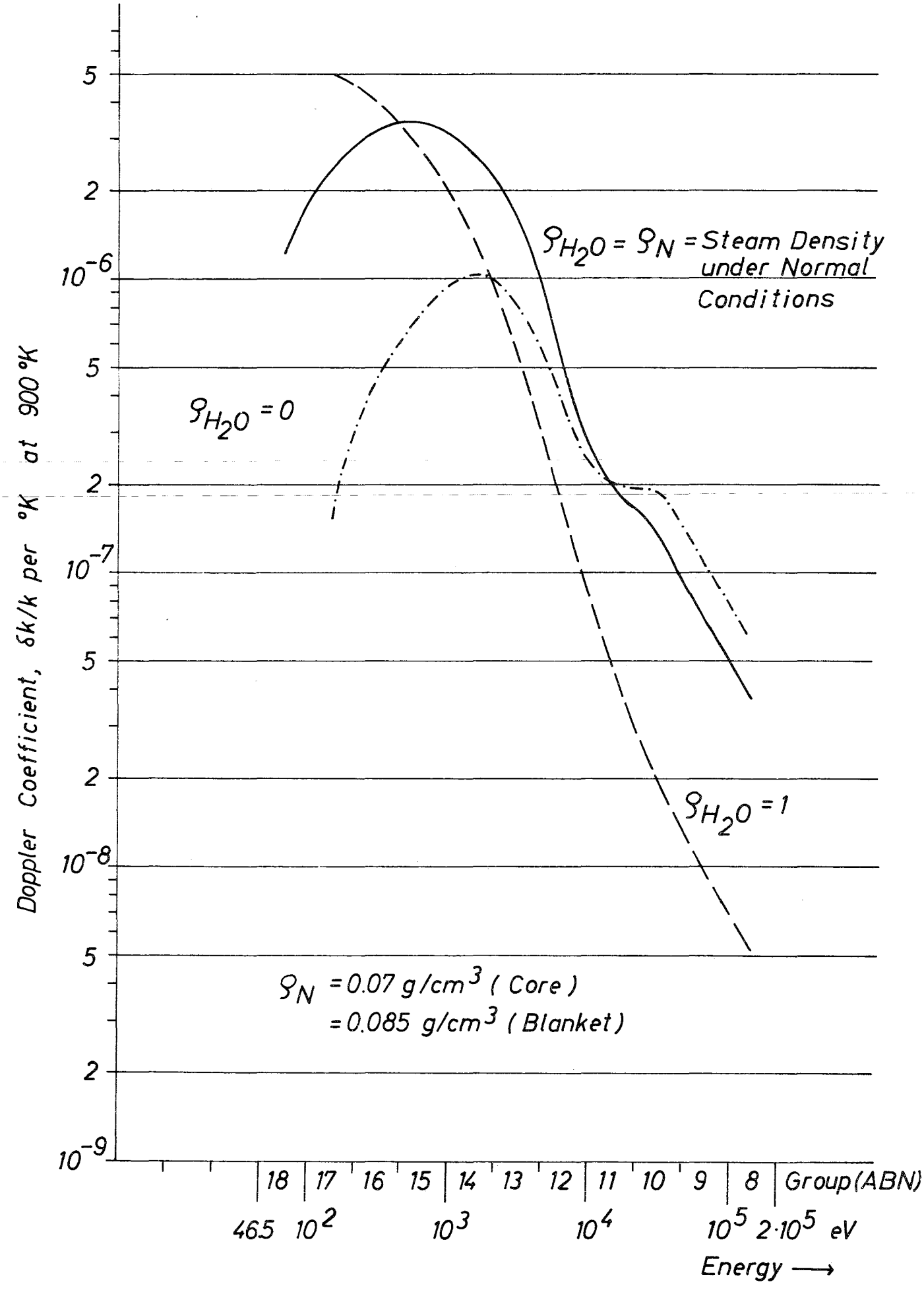

Fig. 19 Calculated Energy Group Contributions to the Doppler Effect of the SNEAK 3 Plutonium Reactor at 900°K